



**HAL**  
open science

## **Hunga Tonga-Hunga Ha'apai Volcano Impact Model Observation Comparison (HTHH-MOC) Project: Experiment Protocol and Model Descriptions**

Yunqian Zhu, Hideharu Akiyoshi, Valentina Aquila, Elisabeth Asher, Ewa M Bednarz, Slimane Bekki, Christoph Brühl, Amy H Butler, Parker Case, Simon Chabrillat, et al.

► **To cite this version:**

Yunqian Zhu, Hideharu Akiyoshi, Valentina Aquila, Elisabeth Asher, Ewa M Bednarz, et al.. Hunga Tonga-Hunga Ha'apai Volcano Impact Model Observation Comparison (HTHH-MOC) Project: Experiment Protocol and Model Descriptions. 2024. hal-04791827v2

**HAL Id: hal-04791827**

**<https://hal.science/hal-04791827v2>**

Preprint submitted on 21 Nov 2024

**HAL** is a multi-disciplinary open access archive for the deposit and dissemination of scientific research documents, whether they are published or not. The documents may come from teaching and research institutions in France or abroad, or from public or private research centers.

L'archive ouverte pluridisciplinaire **HAL**, est destinée au dépôt et à la diffusion de documents scientifiques de niveau recherche, publiés ou non, émanant des établissements d'enseignement et de recherche français ou étrangers, des laboratoires publics ou privés.



Distributed under a Creative Commons Attribution 4.0 International License



# 1 Hunga Tonga-Hunga Ha'apai Volcano Impact Model 2 Observation Comparison (HTHH-MOC) Project: 3 Experiment Protocol and Model Descriptions

4  
5 Yunqian Zhu<sup>1,2</sup>, Hideharu Akiyoshi<sup>3</sup>, Valentina Aquila<sup>4</sup>, Elisabeth Asher<sup>1,5</sup>, Ewa M. Bednarz<sup>1,2</sup>,  
6 Slimane Bekki<sup>6</sup>, Christoph Brühl<sup>7</sup>, Amy H. Butler<sup>2</sup>, Parker Case<sup>8</sup>, Simon Chabrillat<sup>9</sup>, Gabriel  
7 Chiodo<sup>10</sup>, Margot Clyne<sup>11,12</sup>, Lola Falletti<sup>6</sup>, Peter R. Colarco<sup>8</sup>, Eric Fleming<sup>8,13</sup>, Andrin  
8 Jörimann<sup>10,36</sup>, Mahesh Kovilakam<sup>15</sup>, Gerbrand Koren<sup>16</sup>, Ales Kuchar<sup>17</sup>, Nicolas Lebas<sup>14</sup>, Qing  
9 Liang<sup>8</sup>, Cheng-Cheng Liu<sup>12</sup>, Graham Mann<sup>18</sup>, Michael Manyin<sup>8,13</sup>, Marion Marchand<sup>6</sup>, Olaf  
10 Morgenstern<sup>19,20\*</sup>, Paul Newman<sup>8</sup>, Luke D. Oman<sup>8</sup>, Freja F. Østerstrøm<sup>21,22</sup>, Yifeng Peng<sup>23</sup>,  
11 David Plummer<sup>24</sup>, Ilaria Quaglia<sup>25</sup>, William Randel<sup>25</sup>, Samuel Rémy<sup>26</sup>, Takashi Sekiya<sup>27</sup>,  
12 Stephen Steenrod<sup>8,28</sup>, Timofei Sukhodolov<sup>36</sup>, Simone Tilmes<sup>25</sup>, Kostas Tsigaridis<sup>29,30</sup>, Rei  
13 Ueyama<sup>31</sup>, Daniele Visoni<sup>32</sup>, Xinyue Wang<sup>11</sup>, Shingo Watanabe<sup>27</sup>, Yousuke Yamashita<sup>3</sup>, Pengfei  
14 Yu<sup>33</sup>, Wandu Yu<sup>34</sup>, Jun Zhang<sup>25</sup>, Zhihong Zhuo<sup>35</sup>

- 15
- 16 1. Cooperative Institute for Research in Environmental Sciences (CIRES), University of
- 17 Colorado Boulder, USA
- 18 2. NOAA Chemical Sciences Laboratory, Boulder, USA
- 19 3. National Institute for Environmental Studies, Tsukuba, Japan
- 20 4. American University, Department of Environmental Science, Washington, DC, USA
- 21 5. NOAA Global Monitoring Laboratory, Boulder, USA
- 22 6. LATMOS, UVSQ, CNRS, INU, Sorbonne Université, Paris, France
- 23 7. Max Planck Institute for Chemistry, Mainz, Germany
- 24 8. NASA Goddard Space Flight Center, Maryland, USA
- 25 9. Royal Belgian Institute for Space Aeronomy (BIRA-IASB), Brussels, Belgium
- 26 10. Institute for Particle Physics and Astrophysics, ETH Zürich, Switzerland
- 27 11. Department of Atmospheric and Oceanic Sciences, University of Colorado Boulder, Boulder,
- 28 USA
- 29 12. LASP, University of Colorado Boulder, Boulder, USA
- 30 13. Science Systems and Applications, Inc., Lanham, MD, USA
- 31 14. LOCEAN/IPSL, Sorbonne Université, CNRS, IRD, MNHN, Paris, France
- 32 15. NASA Langley Research Center, VA, USA
- 33 16. Copernicus Institute of Sustainable Development, Utrecht University, Utrecht, Netherlands
- 34 17. BOKU University, Vienna, Austria
- 35 18. School of Earth and Environment, University of Leeds
- 36 19. National Institute of Water and Atmospheric Research (NIWA), Wellington, New Zealand
- 37 20. School of Physical and Chemical Sciences, University of Canterbury, Christchurch, New
- 38 Zealand
- 39 21. School of Engineering and Applied Sciences, Harvard University, Cambridge, MA, USA
- 40 22. Department of Chemistry, University of Copenhagen, Copenhagen, Denmark
- 41 23. Lanzhou University, Lanzhou, China
- 42 24. Climate Research Division, Environment and Climate Change Canada, Montréal, Canada
- 43 25. NCAR ACOM, Boulder, USA
- 44 26. HYGEOS, Lille, France



- 45 27. Japan Agency for Marine-Earth Science and Technology (JAMSTEC), Yokohama, Japan  
46 28. University of Maryland-Baltimore County, Baltimore, MD, USA  
47 29. Center for Climate Systems Research, Columbia University, New York, NY, USA.  
48 30. NASA Goddard Institute for Space Studies, New York, NY, USA.  
49 31. NASA Ames Research Center, Moffett Field, CA  
50 32. Department of Earth and Atmospheric Sciences, Cornell University, Ithaca, NY  
51 33. Jinan University, Guangzhou, China  
52 34. Lawrence Livermore National Laboratory, USA  
53 35. Department of Earth and Atmospheric Sciences, University of Quebec in Montreal, Montreal  
54 (Quebec), Canada  
55 36. Physikalisch-Meteorologisches Observatorium Davos and World Radiation Center, Davos,  
56 Switzerland

57

58

59 \* now at: German Meteorological Service (DWD), Offenbach, Germany

60

61

62 Correspondence to: Yunqian Zhu [yunqian.zhu@colorado.edu](mailto:yunqian.zhu@colorado.edu)

63

#### 64 **Abstract:**

65

66 The 2022 Hunga volcanic eruption injected a significant amount of water vapor and a moderate  
67 amount of sulfur dioxide into the stratosphere causing observable responses in the climate  
68 system. We have developed a model-observation comparison project to investigate the evolution  
69 of volcanic water and aerosols, and their impacts on atmospheric dynamics, chemistry, and  
70 climate, using several state-of-the-art chemistry climate models. The project goals are: 1.  
71 Evaluate the current chemistry-climate models to quantify their performance in comparison to  
72 observations; and 2. Understand atmospheric responses in the Earth system after this exceptional  
73 event and investigate the potential impacts in the projected future. To achieve these goals, we  
74 designed specific experiments for direct comparisons to observations, for example from balloons  
75 and the Microwave Limb Sounder satellite instrument. Experiment 1 is a free-running ensemble  
76 experiment from 2022 to 2031. Experiment 2 is a nudged-run experiment from 2022 to 2023  
77 using observed meteorology. To allow participation of more climate models with varying  
78 complexities of aerosol simulation, we include two sets of simulations in Experiment 2:  
79 Experiment 2a is designed for models with internally-generated aerosol while Experiment 2b is  
80 designed for models using prescribed aerosol surface area density. We take model results from  
81 the previously developed Tonga-MIP to fulfill Experiment 3, which focuses on the initial  
82 dispersion and microphysical evolution of aerosol and water plumes. Experiment 4 is designed to  
83 understand the climate impact on the mesosphere from 2022-2027, for which the experiment  
84 design is the same as Experiment 1 but for models that resolve the upper stratosphere and  
85 mesosphere.

86

87

#### 88 **1. Introduction and motivations of this project**

89



90 The Hunga Tonga-Hunga Ha'apai (HTHH) Impacts activity was established in the World  
91 Climate Research Programme (WCRP) Atmosphere Processes And their Role in Climate  
92 (APARC) as a limited-term focused cross-activity with a duration of three years. It aims to assess  
93 the impacts of the 15 January 2022 Hunga volcanic eruption and produce an assessment to  
94 document the Hunga impact on the climate system. The Hunga eruption injected an  
95 unprecedented amount of water (H<sub>2</sub>O) and moderate sulfur dioxide (SO<sub>2</sub>) into the stratosphere  
96 (Millan et al., 2022), presenting a unique opportunity to understand the impacts on the  
97 stratosphere of a large-magnitude explosive phreatomagmatic eruption. The wide range of  
98 satellite observations of the stratospheric water and sulfate plumes, global transport and  
99 dispersion of volcanic materials, and unusual chemical and temperature signals are helpful in  
100 assessing model representations of stratospheric chemistry, aerosol, and dynamics. For example,  
101 the Aura Microwave Limb Sounder (MLS) observed ~150 Tg of water injected by the Hunga  
102 eruption (Millan et al., 2022), which slowly decayed due to the polar stratospheric cloud (PSC)  
103 dehydration process and stratosphere-troposphere exchange (Fleming et al., 2024; Zhou et al.,  
104 2024). Large aerosol optical depth are observed by Ozone Mapping and Profiler Suite (OMPS)  
105 (Taha et al., 2022), due to fast formation of sulfate (Zhu et al., 2022) and the high optical  
106 efficiency of Hunga aerosol particles (Li et al., 2024). Unlike the stratospheric warming patterns  
107 observed from previous large volcanic eruptions (El Chichón in 1982 and Pinatubo in 1991),  
108 global stratospheric temperatures decreased by 0.5 to 1.0 K in the first two years following the  
109 Hunga eruption, largely due to radiative cooling from injected water vapor (Randel et al., 2024).  
110 Satellite observations in June, July, August 2022 reveal reduced lower stratospheric ozone (O<sub>3</sub>)  
111 over the SH midlatitudes and subtropics, with high levels near the equator, exceeding previous  
112 variability. These ozone anomalies coincide with a weakening of the Brewer-Dobson circulation  
113 during this period (Wang et al., 2023). Changes in stratospheric winds also influence the  
114 mesosphere, leading to a stronger mesospheric circulation and corresponding temperature  
115 changes (Yu et al., 2023). These observed phenomena provide a unique opportunity to test the  
116 ability of chemistry-climate models to simulate the evolution of volcanic aerosols combined with  
117 such a large amount of water vapor, as well as understand how volcanic water vapor and aerosols  
118 modify radiative balances and stratospheric ozone.

119 The APARC HTHH Impacts activity aims to provide a benchmark analysis of the  
120 eruption impacts so far, and projections of eruption climate impacts over the next few years. To  
121 facilitate the success of this activity, we designed a multi-model evaluation project, the Hunga  
122 Tonga-Hunga Ha'apai Volcano Impact Model Observation Comparison (HTHH-MOC) Project.  
123 The HTHH-MOC provides a foundation for a coordinated multi-model evaluation of global  
124 chemistry-climate models' performance in response to the Hunga volcanic eruption. It defines a  
125 set of perturbation experiments, where volcanic forcings—injected water vapor and aerosol  
126 concentrations—are consistently applied across participating model members. HTHH-MOC  
127 aims to assess how reliably global chemistry-climate models simulate the climate responses to  
128 this unprecedented volcanic forcing. This project enhances our confidence in attributing and  
129 interpreting observations following the Hunga eruption. The scientific questions related to the  
130 HTHH-MOC are: How does the Hunga volcanic plumes' transport relate to or impact  
131 stratospheric dynamics (such as Brewer-Dobson circulation, polar vortex and the Quasi-Biennial  
132 Oscillation) and upper atmosphere? What are the chemical impacts of the Hunga eruption in the  
133 stratosphere and mesosphere? What and how long is the radiative effect of the Hunga eruption?  
134 Does Hunga impact the tropospheric/surface climate?



135 Therefore, the HTHH-MOC project is focused on evaluating global chemistry-climate  
136 models regarding the following three science themes: (1) plume evolution, dispersion, and large-  
137 scale transport; (2) impacts on stratospheric chemistry and the ozone layer; and (3) radiative  
138 forcing from the eruption and surface climate impacts. Besides the HTHH-MOC project, the  
139 assessment also includes analysis of observations and models that are not global climate models.  
140 In the following paragraph, we describe the HTHH-MOC experiment design and participating  
141 models.  
142

## 143 2. Experiment Design

144 There are four experiments designed to fulfill the scientific goals. Each experiment  
145 includes four kinds of simulations with different volcanic injections, to explore the separate  
146 impacts of volcanic water and aerosols during the post-eruption period: a) Control case (no  
147 eruption); b) H<sub>2</sub>O (~150 Tg) & SO<sub>2</sub> (0.5 Tg); c) Only H<sub>2</sub>O (~150 Tg). d) Only SO<sub>2</sub> (0.5 Tg).  
148 Simulations with the injection of SO<sub>2</sub> only (d) are optional and designed for aerosol-focused  
149 models. The SO<sub>2</sub> and water injections are prescribed based on Millan et al. (2022) and Carn et al.  
150 (2023). Note that ~150 Tg of water is not the injection amount but the amount retained after the  
151 first couple of days. This is because some models form ice particles that fall out of the  
152 stratosphere due to large H<sub>2</sub>O supersaturation during the initial injection (Zhu et al., 2022); these  
153 models will have to inject more H<sub>2</sub>O to counterbalance the ice formation (see **Table 7**). The only  
154 requirement is that the model should have reasonable comparison to the MLS observations for  
155 water vapor as shown in **Figure 1**. Aside from retaining ~150 Tg of water, the water vapor  
156 enhancement should be near 10 hPa to 50 hPa, and most of the water vapor should be located  
157 between 10°N and 30°S by March 2022.

158 The first experiment (**Exp1**) is a free-running ensemble simulation covering the period  
159 from 2022 to 2031. The experiment has been designed to answer questions on: 1. Understanding  
160 the long-term evolution of Hunga water vapor and aerosols in free-running models; 2.  
161 Quantifying Hunga effects on stratospheric temperatures, dynamics, and transport; 3.  
162 Understanding the impact of dynamic changes on ozone chemistry; 4. Quantifying the net  
163 radiative forcings; 5. Estimating surface impacts (e.g., temperature, El Niño-Southern  
164 Oscillation, monsoon precipitation, etc.). Simulations with free-running meteorology are  
165 required to properly understand the impacts of the eruption on atmospheric dynamics and  
166 transport processes, and the resulting impacts of those on chemical species (e.g., ozone) and  
167 surface climate. Since coupling of the atmosphere with ocean and land processes is required to  
168 fully simulate many aspects of the surface impacts, the use of coupled atmosphere, ocean, and  
169 land models is recommended. However, since such a fully interactive set up imposes additional  
170 computing requirements, an alternative model set up with fixed sea-surface temperatures (SSTs)  
171 and sea-ice is also allowed. In that case, the prescribed climatological SSTs and sea-ice data are  
172 obtained by averaging SST during the past decade (2012-2021), with the same data imposed in  
173 both the H<sub>2</sub>O+SO<sub>2</sub> (b) and control (a) simulations. It is important to note that both initial and  
174 boundary conditions in a model come with uncertainties, and model processes are simplified.  
175 Therefore, model simulations are influenced by the characteristics of the model itself and the  
176 background state of the atmospheric system (Jones et al. , 2016; Brodowsky et al., 2021). To  
177 address some of the inherent uncertainties and reduce contribution of interannual variability to  
178 the forced response, we use a large ensemble of simulations with slightly varied initial  
179 conditions.



180 Since some aspects of the response, e.g., impacts on the radiative forcing, may be too  
181 noisy from free-running model simulations even with large ensembles, we have also designed the  
182 second experiment which uses nudged temperature and meteorology to reduce the contribution  
183 of interannual variability and thus isolate chemical changes and their radiative forcing.  
184 Experiment 2 (**Exp2**) is a two-year simulation that runs from 2022 to 2023 with nudged winds  
185 and/or temperature to answer questions on H<sub>2</sub>O and aerosol evolution; quantification of the net  
186 radiative forcings; and impacts on mid-latitude and polar ozone chemistry. **Exp2** has two distinct  
187 realizations: Experiment 2a (**Exp2a**) and Experiment 2b (**Exp2b**). The models participating in  
188 **Exp2a** all have a prognostic aerosol module, but vary in the complexity of their representation of  
189 aerosol microphysics (i.e., bulk, modal, or sectional). Models participating in **Exp2b** use  
190 prescribed aerosol surface area density (SAD) and radiative properties as input to the models  
191 (Jörmann et al., 2024). The prescribed aerosol properties are calculated using Global sSpace-  
192 based Stratospheric Aerosol Climatology (GloSSAC; Thomason et al., 2018; Kovilakam et al.,  
193 2020, 2023) version 2.22 aerosol data from 1979-2023. Note that for the period after the Hunga  
194 eruption, GloSSAC uses the Stratospheric Aerosol and Gas Experiment (SAGEIII/ISS) version  
195 5.3 interpolated along the time axis and the Optical Spectrograph and InfraRed Imager System  
196 (OSIRIS) version 7.3 to fill in any missing data poleward of 60° N/S due to the unavailability of  
197 the Cloud-Aerosol Lidar and Infrared Pathfinder Satellite Observations (CALIPSO) data since  
198 January 2022. Therefore, when conducting analyses north/south of 60° N/S it should be noted that  
199 the aerosols may be underestimated due to the OSIRIS instrument retrieval biases. We ask for  
200 the models to check their initial chemical fields against MLS to see if the models are qualified to  
201 evaluate their ozone chemistry. The nudged runs of **Exp2** enable isolation of the chemical impact  
202 of the Hunga eruption from the volcanically induced changes in dynamics by comparing the runs  
203 with and without H<sub>2</sub>O+SO<sub>2</sub> injection. The net radiative effect anomaly due to water and sulfate  
204 aerosol can also be calculated by comparing the control run (a) with the H<sub>2</sub>O+SO<sub>2</sub> injection run  
205 (b).

206 The third experiment (**Exp3**) is designed to explore the plume evolution between 1 day  
207 and up to 1 or 2 months after the eruption, including plume microphysics and chemistry. This  
208 experiment is adopted from TongaMIP (designed by Clyne et al., 2024), which has both free-  
209 running and nudged simulations to study the Hunga plume during the first three months after the  
210 eruption. All models are requested to inject 150 Tg of water but the retaining of the water varies  
211 between models, while other experiments here ask to retain ~150 Tg of water in the stratosphere.  
212 This is because for other experiments, our goal is to reproduce the long-term observations first  
213 and then to understand the Hunga climate impact; while **Exp3** is designed to understand the  
214 differences in physics processes (i.e., cloud and aerosol physics and sulfur chemistry) between  
215 models, expanding on findings from prior model intercomparison (Clyne et al., 2021; Quaglia et  
216 al., 2023) with upgraded and additional models. These experiments are detailed in Clyne et al.  
217 (2024).

218 The fourth experiment (**Exp4**) is a free-running ensemble simulation to understand  
219 climate impacts on the mesosphere and ionosphere from 2022-2027, such as gravity wave drag,  
220 temperature changes, polar mesospheric clouds (PMCs), and atmospheric circulation. This  
221 experiment uses the first 5 years of **Exp1** and is limited to the models resolving the upper  
222 atmosphere.

223 **Table 1** shows the forcings and emissions data used for all experiments except for  
224 Experiment 3 (**Exp3**). **Table 2** shows the settings specific to each experiment. For volcanic  
225 injection for **Exp1, 2** and **4**, we recommend the injections of H<sub>2</sub>O and SO<sub>2</sub> at 4 UTC on Jan 15,





226 2022. All the models are required to retain a similar amount of water as observed by MLS (~ 150  
 227 Tg). The models are recommended to compare with the MLS evolution for validation (**Figure 1**).  
 228 The goal is to retain the same amount of water and similar altitude to start with, so we can  
 229 analyze the water's impact on the stratosphere and climate. If injecting 25-30 km cannot retain  
 230 150 Tg, models can inject higher than 30 km. The SO<sub>2</sub> injection is required to be 0.5 Tg for all  
 231 models. The injection locations are not required to be co-injected with H<sub>2</sub>O.

232 The data analysis of this project is designed to do inter-model comparisons, as well as  
 233 inter-experiment comparisons. For example, the comparisons between **Exp2a** and **Exp2b** can  
 234 help to understand how well we simulate the sulfate SAD and the importance of SAD variation  
 235 for stratospheric ozone chemistry. Comparing **Exp1** and **Exp2** for the same period can help  
 236 understand radiative forcing and radiative effects. In addition, large (10-20) member ensembles  
 237 are requested for free-running simulations to better quantify the role of internal variability in the  
 238 climate response.

239  
 240

**Table 1. Summary of forcings and emissions data used in each experiment.**

Spin-up*	5 years nudged runs
Degassing** and eruptive volcano source	Need both degassing and eruptive volcanic input for 5 year spin-up. Degassing continues during the experiment runs (e.g. 10 years for <b>Exp1</b> , 2 years for <b>Exp2</b> ). recommended references: Volcanic degassing Carn et al. (2017); Eruptive volcanoes (Neely III, & Schmidt (2016) <a href="https://archive.researchdata.leeds.ac.uk/96/">https://archive.researchdata.leeds.ac.uk/96/</a> or Carn et al. (2017); Assume no more explosive volcanoes after Hunga.
Surface emission	Coupled Model Intercomparison Project phase 6 (CMIP6) emissions follow SSP2-4.5 (Gidden et al., 2019), which adopts an intermediate greenhouse gas (GHG) emissions: CO <sub>2</sub> emissions around current levels before beginning to decline by 2050.
Chemical initialization	Stratospheric chemistry fields (such as O <sub>3</sub> , H <sub>2</sub> O) at the beginning of 2022 should be compared with MLS observations for validation if the model participates in evaluation of the Hunga stratospheric chemistry impact.

241 \* 5 years is enough to reach sulfate equilibrium in the stratosphere; water may take 7 years (each model  
 242 should adjust the spin-up time according to model features). \*\* Recommended degassing volcanic  
 243 emissions injected at the cone altitude, constant flux based on Carn et al. (2017). Database is updated  
 244 through 2022 here: <https://doi.org/10.5067/MEASURES/SO2/DATA406>.

245  
 246

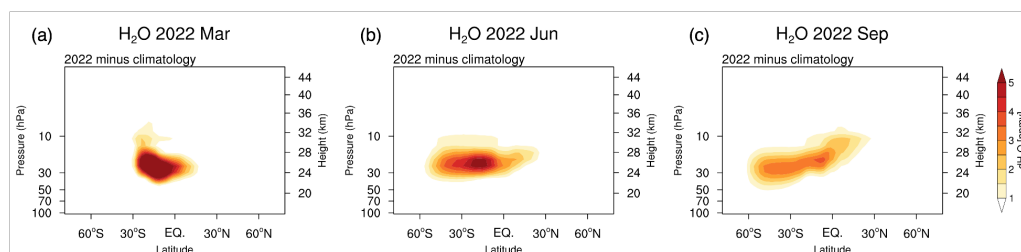
**Table 2. Experiment design**

Experiment	Meteorology	period	aerosol treatment	QBO	SST	Ensemble members
Exp1	Free run starts Feb 1.	10 years 2022-2031	model simulated aerosol or	Internal generated (Nudge if model doesn't generate)	Fixed (climatology = mean of monthly average during the past decade (2012-2021), repeating annually) This applies to spin-up time too.	10-20
	(i.e. nudge until Jan 31)		prescribed		Coupled ocean (optional) initialize with observed ocean state (see section 3 for individual model descriptions)	10-20
Exp2a	Nudged wind only and/or nudged T and wind*	2 years 2022-2023	model simulated aerosol	nudged	Observed SST	-



Exp2b	Nudged wind only and/or nudged T and wind*	2 years 2022-2023	prescribed	nudged	Observed SST	-
Exp3 (Tonga-MIP)	Both free run and nudged runs are conducted	3 months after the eruption	model simulated aerosol	not specified	not specified	-
Exp4	same as Exp1	5 years 2022-2027	same as Exp1	same as Exp1	same as Exp1	same as Exp1

247  
248  
249



250  
251  
252  
253  
254

**Figure 1.** Monthly average water vapor perturbation after the Hunga eruption from MLS. Panels (a-c) show the observed dispersion of the H<sub>2</sub>O enhancement in 2022 in the months of (a) March, (b) June, and (c) September.

### 3. Model output

255  
256  
257  
258  
259  
260  
261  
262  
263  
264  
265  
266

The model output covers variables based on the Chemistry-Climate Modeling Initiative (CCMI) output list with some additions specific to this study. The detailed list is provided in the **Supplementary Excel Table**. We have requested that all models generate the same variable names, units, ordering of dimensions (longitude from 0°E to 360°E; latitude from 90°S to 90°N; pressure levels from 1000 hPa to 0.03 hPa or altitude from 0 meter to 85,000 meter), and file name structure (e.g. ‘variable\_domain\_modelname\_experimentname.nc’ or ‘domain\_modelname\_experimentname.variable.nc’). The examples of Experiment\_name are: HTHHMOC-Exp1, HTHHMOC-Exp1and4. The example file names are: Monthlymean\_WACCM6MAM\_HTHHMOC-Exp1and4-NoVolc-fixedSST.ensemble001.O3.nc or O3\_Dailymean\_WACCM6MAM\_HTHHMOC-Exp1and4-H2Oonly-fixedSST.ensemble001.nc.

267  
268  
269  
270  
271

The 3D model output is requested on both model levels (hybrid pressure or height) and interpolated to CMIP6 plev39 grid (plev39: 1000, 925, 850, 700, 600, 500, 400, 300, 250, 200, 170, 150, 130, 115, 100, 90, 80, 70, 50, 30, 20, 15, 10, 7, 5, 3, 2, 1.5, 1.0, 0.7, 0.5, 0.4, 0.3, 0.2, 0.15, 0.1, 0.07, 0.05, 0.03 hPa) and for Mesospheric analysis (**Exp4**) adding 0.02, 0.01, 0.007, 0.005, 0.003, 0.001 above the plev39 grid.

272  
273  
274  
275

Monthly mean output is requested for all variables for both **Exp1** and **Exp4**, with some fields (specified in the Excel sheet) as daily mean. Some of the fields requested as daily means are specified, either as surface fields or at reduced number of pressure levels. Daily mean output is requested for all variables for **Exp2**.





276 The model output (~33 TB) is archived at the JASMIN workspace (jasmin.ac.uk).  
277 JASMIN provides large storage space and compute facilities to facilitate the data archiving and  
278 post data analysis of this project. This reduces the need for data transfers and allows reproducible  
279 computational workflows. Seddon et al (2023) described the facility in detail. Our next phase is  
280 to publicly release the data by transferring the data to the Centre for Environmental Data  
281 Analysis (CEDA) archiving system.

282

#### 283 4. Model Descriptions and the Hunga Volcanic Injection Specification

284

285 As part of the three-year Hunga Impact activity, this project is highly time-sensitive. We  
286 designed the timeline for each experiment (**Figure 2**) to facilitate the completion of the 2025  
287 Hunga Impact assessment. However, the JASMIN workspace will remain open for the uploading  
288 of modeling data after the deadline denoted in **Figure 2** until 2025.

289

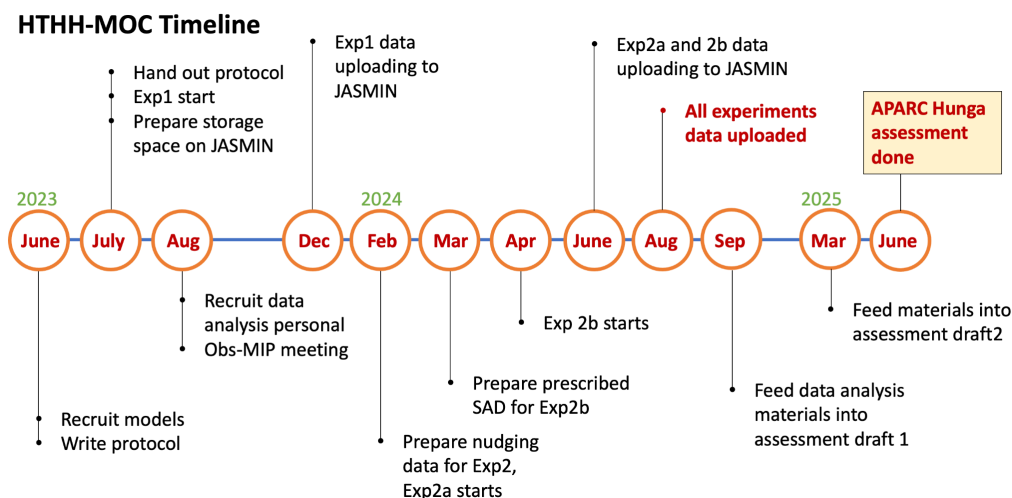
290 This paper only includes model descriptions for those models that submitted the output  
291 following the assessment timeline. The model setup follows the protocols listed in Section 2  
292 unless specified below. **Tables 4-7** provide key information on the participant models, which are  
293 detailed described in the following paragraphs for each model.

294

295 Three models participated only in **Exp3** (Tonga-MIP) and not in the other experiments:  
296 for the descriptions of these three models (MIROC-ES2H, SOCOLv4, and GA4 UM-UKCA) we  
297 refer to Clyne et al. (2024).

298

299



296

297

298

299

**Figure 2.** The timeline designed for HTHH-MOC in order to cooperate with the APARC HTHH Impact assessment.



300 **Table 4. Participating models and contact information**

Model name	Description reference paper	Institutions (that develop the model)	Primary contact (who runs the model)	Emails
CAM5/CARMA	Yu et al. (2015)	CU Boulder Jinan Univ.	Pengfei Yu Yifeng Peng	<a href="mailto:pengfei.yu@colorado.edu">pengfei.yu@colorado.edu</a> <a href="mailto:pengvf16@lzu.edu.cn">pengvf16@lzu.edu.cn</a>
CCSRNIES-MIROC3.2	Akiyoshi et al. (2023), Akiyoshi et al. (2016)	NIES	Yosuke Yamashita Hideharu Akiyoshi	<a href="mailto:yamashita.yosuke@nies.go.jp">yamashita.yosuke@nies.go.jp</a> <a href="mailto:hakiyosi@nies.go.jp">hakiyosi@nies.go.jp</a>
CMAM	Jonsson et al. (2004), Scinocca et al. (2008)	CCCma, Environment and Climate Change Canada	David Plummer	<a href="mailto:david.plummer@ec.gc.ca">david.plummer@ec.gc.ca</a>
EMAC MPIC	Schallock et al. (2023)	MPI-C, -M, DLR	Christoph Brühl	<a href="mailto:christoph.bruehl@mpic.de">christoph.bruehl@mpic.de</a>
GA4 UM-UKCA	Dhomse et al. (2020)	Univ. Leeds	Graham Mann, Sandip Dhomse	<a href="mailto:G.W.Mann@leeds.ac.uk">G.W.Mann@leeds.ac.uk</a> , <a href="mailto:S.S.Dhomse@leeds.ac.uk">S.S.Dhomse@leeds.ac.uk</a>
GEOSCCM	Nielsen et al. (2017)	NASA	Peter Colarco	<a href="mailto:peter.r.colarco@nasa.gov">peter.r.colarco@nasa.gov</a>
GEOS/CARMA	Nielsen et al. (2017)	NASA	Parker Case	<a href="mailto:parker.a.case@nasa.gov">parker.a.case@nasa.gov</a>
GSFC2D	Fleming et al. (2020)	NASA	Eric Fleming	<a href="mailto:eric.l.fleming@nasa.gov">eric.l.fleming@nasa.gov</a>
IFS-COMPO Cy49R1	Huijnen et al. (GMD, 2016), Rémy et al. (GMD, 2022)	ECMWF and team CAMS2_35	Simon Chabrilat Samuel Rémy	<a href="mailto:Simon.chabrilat@aeronomie.be">Simon.chabrilat@aeronomie.be</a> <a href="mailto:sr@hygeos.com">sr@hygeos.com</a>
LMZ6.2-LR-STRATAER/LMD Z6.2-LR-STRATAER-REPROBUS	O. Boucher et al. 2020, Marchand et al., 2012	CNRS, Sorbonne Université, IPSL, LATMOS, LOCEAN	Marion Marchand, Slimane Bekki, Nicolas Lebas, Lola Falletti	<a href="mailto:marion.marchand@latmos.ipsl.fr">marion.marchand@latmos.ipsl.fr</a> , <a href="mailto:slimane.bekki@latmos.ipsl.fr">slimane.bekki@latmos.ipsl.fr</a> , <a href="mailto:nicolas.lebas@locean.ipsl.fr">nicolas.lebas@locean.ipsl.fr</a> , <a href="mailto:lola.falletti@latmos.ipsl.fr">lola.falletti@latmos.ipsl.fr</a>
MIROC-CHASER	Sekiya et al. (2016)	JAMSTEC	Shingo Watanabe, Takashi Sekiya	<a href="mailto:wnabe@jamstec.go.jp">wnabe@jamstec.go.jp</a> , <a href="mailto:tsekiya@jamstec.go.jp">tsekiya@jamstec.go.jp</a>
MIROC-ES2H	Tatebe et al. (2019), Kawamiya et al. (2020)	JAMSTEC and NIES	Shingo Watanabe, Takashi Sekiya, Tatsuya Nagashima, Kengo Sudo	<a href="mailto:wnabe@jamstec.go.jp">wnabe@jamstec.go.jp</a> , <a href="mailto:tsekiya@jamstec.go.jp">tsekiya@jamstec.go.jp</a> , <a href="mailto:nagashima.tatsuya@nies.go.jp">nagashima.tatsuya@nies.go.jp</a> , <a href="mailto:kengo@nagoya-u.jp">kengo@nagoya-u.jp</a>
SOCOLv4	Sukhodolov et al. (2021)	PMOD/WRC and ETH-Zurich	Timofei Sukhodolov	<a href="mailto:timofei.sukhodolov@pmodwrc.ch">timofei.sukhodolov@pmodwrc.ch</a>
WACCM6/CARM A	Tilmes et al. (2023)	NCAR	Simone Tilmes Cheng-Cheng Liu Yunqian Zhu Margot Clyne (Exp 3)	<a href="mailto:tilmes@ucar.edu">tilmes@ucar.edu</a> <a href="mailto:chengcheng.liu@lasp.colorado.edu">chengcheng.liu@lasp.colorado.edu</a> <a href="mailto:yunqian.zhu@noaa.gov">yunqian.zhu@noaa.gov</a> <a href="mailto:margot.clyne@colorado.edu">margot.clyne@colorado.edu</a>
WACCM6/MAM	Mills et al. (2016)	NCAR	Xinyue Wang Simone Tilmes Jun Zhang Wandi Yu	<a href="mailto:xinyuew@colorado.edu">xinyuew@colorado.edu</a> <a href="mailto:tilmes@ucar.edu">tilmes@ucar.edu</a> <a href="mailto:jzhan166@ucar.edu">jzhan166@ucar.edu</a> <a href="mailto:yu44@llnl.gov">yu44@llnl.gov</a>



Zhihong Zhuo [zhuo.zhihong@uqam.ca](mailto:zhuo.zhihong@uqam.ca)  
 Ewa Bednarz [ewa.bednarz@noaa.gov](mailto:ewa.bednarz@noaa.gov)  
 Margot Clyne (Exp 3) [margot.clyne@colorado.edu](mailto:margot.clyne@colorado.edu)

301  
 302

**Table 5. Participating models for each experiment.**

Model names	Exp1	Exp1/4 (coupled ocean)	Exp2a	Exp2b	Exp3 (Tonga-MIP)	Exp4
CAM5/CARMA			X			
CCSRNIES- MIROC3.2				X		
CMAM	X (H2O- only)					X (H2O-only)
EMAC MPIC			X			
GA4 UM-UKCA					X	
GEOSCCM	X		X		X	
GEOS/CARMA			X			
GSFC2D	X			X		X
IFS-COMPO			X			
LMDZ6.2-LR- STRATAER			X		X	
LMDZ6.2-LR- STRATAER- REPROBUS			X		X	
MIROC- CHASER	X		X			
MIROC-ES2H					X	
SOCOLv4					X	
WACCM6/CAR MA			X		X	
WACCM6/MA M	X	X	X		X	X

303  
 304  
 305  
 306

**Table 6. Model resolutions and schemes used for experiments except for Exp3 (Tonga-MIP)**

Model names	Horizontal resolution	nlevels	Model Top	Vertical resolution in the stratosphere	Aerosol scheme	Specified dynamic source	QBO for free run	Chemistry package (tropospheric chemistry included?)
CAM5/CARM A	~2 deg	56	45 km	1-4 km	CARMA sectional(20 bins)	GEOS5	-	MOZART (yes)
CCSRNIES- MIROC3.2	T42	34	0.01 hPa	1-3 km	None	MERRA-2	nudged	full strat; no tropo
CMAM	T47	80	0.006 hPa	0.8 - 2.5 km	None	ERA5	nudged	stratospheric + methane-NOx in troposphere
EMAC MPIC	T63	90	0.01 hPa	0.5km in LS	GMXE, modal	ERA-5	Internal but slightly nudged	MECCA, simplified troposphere



GEOSCCM	c90 (~1 deg)	72	0.01 hPa	~1 km	GOCA RT (Bulk)	MERR A-2/GEOS-FP	Internal generated	GMI (yes)
GEOS/CARMA	c90 (~1 deg)	72	0.01 hPa	~1 km	CARMA (sectional 24 bins)	MERR A-2/GEOS-FP	Internal generated	GMI (yes)
GSFC2D	4°	76	.002 hPa (~92 km)	1km	Prescribed only	MERR A-2	Internal generated	full strat; partial trop
IFS-COMPO	T1,511 (~40km)	137	0.01 hPa	0.5-1.5 km	Bulk	ERA5	-	BASCOE (strato) + CB05 (tropo)
LMDZ6.2-LR-STRATAER	2.5° × 1.3°	79	80k m	1-5 km	S3A(sectional 36 bins)	ERA5	Internal generated	No
LMDZ6.2-LR-STRATAER-REPROBUS	2.5° × 1.3°	79	80k m	1-5 km	S3A(sectional 36 bins)	ERA5	Internal generated	REPROBUS
MIROC-CHASER	T85	81	0.004 hPa	0.7-1.2 km	MAM 3	MERR A-2	Internal generated	troposphere-stratosphere chemistry
WACCM6/CARMA	~1 deg	70	140 km	1-2 km	Sectional (20 bins)	MERRA-2	Internal generated	MOZART (yes)
WACCM6/MAM	~1 deg	70	140 km	1-2 km	MAM4	MERRA-2	Internal generated	MOZART (yes)

307  
 308  
 309

**Table 7. Hunga volcanic injection profile for experiments except for Exp3 (Tonga-MIP)**

Model names	Data and duration	H <sub>2</sub> O amount (left after a week)	H <sub>2</sub> O altitude	H <sub>2</sub> O location/area	SO <sub>2</sub> amount	SO <sub>2</sub> altitude	SO <sub>2</sub> location/area
CAM5/CARMA	Jan 15, 6 hrs	150 Tg (~135 Tg)	25-35 km	22-14°S, 182-186°E	0.5 Tg	20-28 km	22-14°S, 182-186°E
CCSRNIES-MIROC3.2	Jan 15, instantly	150 Tg (~150 Tg)	12.0-27.6 hPa	181.4–187.0°E, 14.0–22.3°S	-	-	-
CMAM	Feb 20, 5 days	150 Tg (~150 Tg)	near 25.5 km	zonally average	-	-	-
EMAC MPIC	Jan 16, 12hrs	136 Tg (~130 Tg)	Gaussian centered at 21.5hPa	23-19°S, 177-173°W	0.4 Tg based on obs.	23-27 km based on obs.	30°S-5°N, 90-120°W (330°)
GEOSCCM	Jan 15, 6 hrs	750 Tg (~150 Tg)	25-30 km	22-14°S, 182-186°E	0.5 Tg	25-30 km	22-14°S, 182-186°E



GEOS/CARMA	Jan 15, 6 hrs	750 Tg (~150 Tg)	25-30 km	22-14°S, 182-186°E	0.5 Tg	25-30 km	22-14°S, 182-186°E
GSFC2D	use MLS H <sub>2</sub> O profile until March 1	~150 Tg (~150 Tg)	-	zonally average	-	-	-
IFS-COMPO	Jan 15, 3 hrs	190 Tg (~150 Tg)	25-30 km	400 km by 200 km centered 20°S and 175°W	0.5 Tg	25-30 km	400 km by 200 km centered 20°S and 175°W
LMDZ6.2-LR-STRATAER	Jan 15, 1 day	150 Tg (~150 Tg)	Gaussian centered at 27.5 km and standard deviation of 2.5 km	22°-14°S, 182-186°E	0.5 Tg	Gaussian centered at 27.5 km and standard deviation of 2.5 km	22-14°S, 182-186°E
LMDZ6.2-LR-STRATAER-REPROBUS	Jan 15, 1 day	150 Tg (~150 Tg)	Gaussian centered at 27.5 km and standard deviation of 2.5 km	22-14°S, 182-186°E	0.5 Tg	Gaussian centered at 27.5 km and standard deviation of 2.5 km	22-14°S, 182-186°E
MIROC-CHASER	Jan 15 4 UTC, 6 hours	186 Tg (~150 Tg)	25-30 km	22-14°S, 182-186°E	0.5 Tg	25-30 km	22-14°S, 182-186°E
WACCM6/CARMA	Jan 15, 6 hours	150 Tg (~135 Tg)	25-35 km	22-14°S, 182-186°E	0.5 Tg	20-28 km	22-14°S, 182-186°E
WACCM6/MAM	Jan 15, 6 hours	150 Tg (~150 Tg)	25-35km	22-6°S, 182.5 -202.5°E	0.5 Tg	26.5-36 km	22-6°S, 182.5 -202.5°E

310

311

#### 312 4.1 CAM5/CARMA

313 The atmospheric component of the Community Atmosphere Model version 5 (CAM5)  
 314 (Lamarque et al., 2012) is the atmospheric component of the Community Earth System Model,  
 315 version 1 (CESM1.2.2, Hurrell et al., 2013), with a top at around 45 km. CAM5 has a horizontal  
 316 resolution of 1.9° latitude × 2.5° longitude, utilizing the finite volume dynamical core (Lin &  
 317 Rood, 1996). The model has 56 vertical levels, with a vertical resolution ~1 km in the upper  
 318 troposphere and lower stratosphere. The modeled winds and temperatures were nudged to the 3-  
 319 hour Goddard Earth Observing System 5 (GEOS-5) reanalysis data set (Molod et al., 2015) every  
 320 time step (30 min) by 1% (i.e., a 50 h Newtonian relaxation time scale). The aerosol is interactively  
 321 simulated using a sectional aerosol microphysics model, the Community Aerosol and Radiation  
 322 Model for Atmospheres (CARMA, Yu et al., 2015). The model uses the Model for Ozone and  
 323 Related Chemical Tracers (MOZART) chemistry that is used for both tropospheric (Emmons et  
 324 al., 2010) and stratospheric chemistry (English et al., 2011; Mills et al., 2016). The volcanic



325 emissions from continuously degassing volcanoes uses the emission inventory RCP8.5 and  
326 FINNv1.5. No volcanic eruptions except the Hunga 2022 eruption are included.

327 The initial volcanic injection altitude and area are determined by validating the water and  
328 aerosol transportation in months shown in **Figure 1** following the tests in Zhu et al. (2022), Wang  
329 et al. (2023) and Zhang et al. (2024). In these simulations, the H<sub>2</sub>O is injected at 25 to 35 km  
330 altitude and SO<sub>2</sub> injected at 20 to 28 km altitude. The injection latitude ranges from 22°S to 14°S,  
331 and longitude ranges from 182°E to 186°E (Zhu et al., 2022). The initial injection of H<sub>2</sub>O is 150  
332 Tg, with ~ 135 Tg left after the first week following the eruption.

333

#### 334 **4.2 CCSRNIES-MIROC3.2**

335 The Center for Climate System Research/National Institute for Environmental Studies -  
336 Model for Interdisciplinary Research on Climate version 3.2 Chemistry Climate Model  
337 (CCSRNIES-MIROC3.2 CCM) (Akiyoshi et al. 2023) was developed based on versions 3.2 of the  
338 MIROC atmospheric general circulation model (AGCM), incorporating a stratospheric chemistry  
339 module that was developed at National Institute for Environmental Studies (NIES) and the  
340 University of Tokyo. The model has a horizontal resolution of T42 (2.8° latitude × 2.8° longitude)  
341 and 34 vertical levels, with a vertical resolution ~1 km in the lower stratosphere/upper troposphere  
342 and ~3 km in the upper stratosphere and mesosphere. The top level is located at 0.01 hPa  
343 (approximately 80 km).

344 The chemistry in the CCSRNIES-MIROC3.2 CCM is a stratospheric chemistry module  
345 including 42 photolysis reactions, 142 gas-phase chemical reactions and 13 heterogeneous  
346 reactions for multiple aerosol types (Akiyoshi et al., 2023). Tropospheric chemistry is not included,  
347 but the stratospheric chemistry scheme is used for both the troposphere and mesosphere.

348 In the CCSRNIES-MIROC3.2 CCM, only **Exp2b** can be performed. The atmospheric  
349 temperature and horizontal winds are nudged toward Modern-Era Retrospective analysis for  
350 Research and Applications Version 2 (MERRA-2) reanalysis (Gelaro et al., 2017) with a 1-day  
351 relaxation using instant values at 6-hour interval (Akiyoshi et al., 2016). The HadISST data is used  
352 during the simulation.

353 The CCSRNIES-MIROC3.2 CCM does not have any microphysics scheme for volcanic  
354 aerosols. The surface area and spectral optical parameters of extinction, single scattering albedo,  
355 and asymmetric factor for Hunga aerosols were prescribed in the model from the GloSSAC version  
356 2.22 aerosol data (Jörmann et al., 2024). H<sub>2</sub>O was injected instantly on 15 January 2022 at the 12  
357 grids of the model in the region 181.4°E–187.0°E in longitude, 14.0°S–22.3°S in latitude, and 12.0  
358 hPa–27.6 hPa in pressure level. A uniform number density of  $1.709 \times 10^{15}$  molecules/cm<sup>3</sup> H<sub>2</sub>O was  
359 injected in each of the 12 grids which amounts to ~150 Tg.

360

#### 361 **4.3 CMAM**

362 The Canadian Middle Atmosphere Model (CMAM) is based on a vertically extended  
363 version of CanAM3.1, the third generation Canadian Atmospheric Model (Scinocca et al., 2008).  
364 Compared to the standard configuration of CanAM3.1, for CMAM the model top was raised to  
365 0.0006 hPa (approximately 95 km) and the parameterization of non-orographic gravity wave  
366 drag (Scinocca, 2003) and additional radiative processes important in the middle atmosphere  
367 (Fomichev et al., 2004) have been included. The gas-phase chemistry includes a comprehensive  
368 description of the inorganic Ox, NO<sub>x</sub>, HO<sub>x</sub>, ClO<sub>x</sub> and BrO<sub>x</sub> families, along with CH<sub>4</sub>, N<sub>2</sub>O, six  
369 chlorine containing halocarbons, CH<sub>3</sub>Br and, to account for an additional 5 ppt of bromine from  
370 short-lived source gases, CH<sub>2</sub>Br<sub>2</sub> and CHBr<sub>3</sub> (Jonsson et al., 2004). A prognostic description of,





371 and associated heterogeneous chemical reactions on water ice PSCs (PSC Type II) and liquid  
372 ternary solution (PSC Type Ib) particles is included, although gravitational settling  
373 (dehydration/denitrification) is not calculated and species return to the gas phase when  
374 conditions no longer support the existence of PSC particles.

375 The simulations for the HTHH-MOC simulations were performed at T47 spectral  
376 resolution (approximately  $3.8^\circ$  resolution on the linear transform grid used for the model  
377 physics), with 80 vertical levels giving a vertical resolution of approximately 0.8 km at 100 hPa,  
378 increasing to 2.3 km above 0.1 hPa. The CMAM does not internally generate a QBO, so the  
379 zonal winds in the equatorial region were nudged towards a dataset based on observed variations  
380 up to December 2023, constructed using the method of Naujokat (1986) and extended into the  
381 future by repeating a historical period that is congruent with the observed QBO in late 2023.  
382 Water vapor from the Hunga eruption was added as a zonally average perturbation to the model  
383 water over five days from 00 UTC on February 20, 2022. The spatial distribution of the anomaly  
384 was designed to reproduce the water vapor anomaly observed in mid-February by the The  
385 Atmospheric Chemistry Experiment - Fourier Transform Spectrometer (ACE-FTS) (Bernath et  
386 al., 2005) satellite (Patrick Sheese, personal communication), with a maximum value of 13.3  
387 ppm at  $17^\circ\text{S}$  and 25.5 km and producing an anomaly of  $\sim 150$  Tg  $\text{H}_2\text{O}$  in the stratosphere.  
388

#### 389 4.4 EMAC MPIC

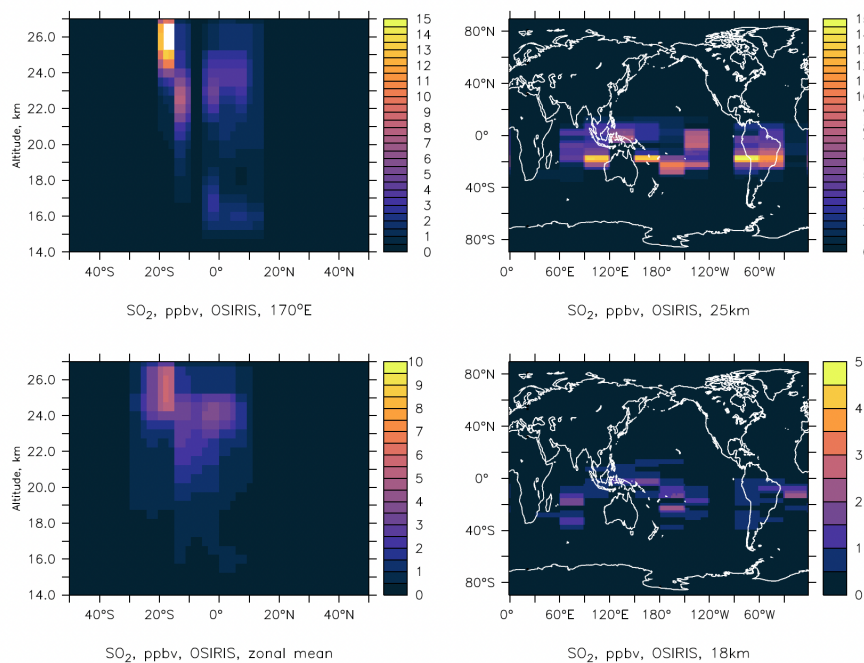
390 The chemistry-climate model EMAC (ECHAM5/MESSy Atmospheric Chemistry)  
391 consists of the European Centre Hamburg general circulation model (ECHAM5) and the  
392 Modular Earth Submodel System (MESSy) (e.g., Jöckel et al., 2010). Here we use the version of  
393 Schallock et al. (2023) in horizontal resolution T63 ( $1.87^\circ \times 1.87^\circ$ ) with 90 levels between the  
394 surface and 0.01 hPa.

395 Vorticity, divergence, and temperatures between boundary layer and 100 hPa are nudged  
396 to the reanalysis ERA5 (Hersbach et al., 2020), as well as surface pressure. SSTs and sea ice  
397 cover are prescribed by ERA5 data. The model can generate an internal QBO but for comparison  
398 with observations it was slightly nudged to the Singapore data compiled by Free University of  
399 Berlin and Karlsruhe Institute of Technology.

400 The model contains gas-phase and heterogeneous chemistry on PSCs and interactive  
401 aerosols. Surface mixing ratios of chlorine- and bromine-containing halocarbons and other long-  
402 lived gases are nudged to Advanced Global Atmospheric Gases Experiment (AGAGE)  
403 observations. The microphysical modal aerosol module contains four soluble and three insoluble  
404 modes for sulfate, nitrate, dust, organic and black carbon, and aerosol water (Pringle et al.,  
405 2010). The instantaneous radiative forcing by tropospheric and stratospheric aerosols can be  
406 calculated online by multiple calls of the radiation module. Volcanoes injecting material into the  
407 stratosphere are considered as in Schallock et al. (2023) using the perturbations of stratospheric  
408  $\text{SO}_2$  observed by the Michelson Interferometer for Passive Atmospheric Sounding (MIPAS) and  
409 aerosol extinction observed by OSIRIS. This method, based typically on data of a 10-day period,  
410 distributes the injected  $\text{SO}_2$  over a larger volume than typical point source approaches using the  
411 same integrated mass (see also Kohl et al., 2024). For Hunga this method has the disadvantage  
412 that  $\text{H}_2\text{O}$  and  $\text{SO}_2$  are not co-injected since  $\text{H}_2\text{O}$  is injected in 12 hours in a slab consisting of  
413 four horizontal boxes and a Gaussian vertical distribution centered at 21.5 hPa. For **Exp2a** we  
414 continue the 30-year transient simulation presented in Schallock et al. (2023) with and without  
415 Hunga Tonga. The simulated  $\text{H}_2\text{O}$ -perturbation is consistent with **Figure 1**. The  $\text{SO}_2$  injection is



416 derived based on the extinction from the OSIRIS observation averaged over about 10 days  
417 (**Figure 3**) (Bruehl et al., 2023).



418  
419 **Figure 3.** The SO<sub>2</sub> perturbation from Hunga derived from extinction observed by OSIRIS  
420 averaged over about 10 days, i.e., including several snapshots of the westward moving plume.  
421 Note that the colorbars are not the same in each panel.

422  
423

#### 424 4.5 GEOSCCM

425 The NASA Goddard Earth Observing System Chemistry-Climate Model (GEOSCCM) is  
426 based on the GEOS Earth system model (Reinecker et al. 2008, Molod et al. 2015). For the  
427 HTHH-MOC experiments the model is run on a cubed-sphere horizontal grid at a C90 resolution  
428 (~100 km) with 72 vertical hybrid-sigma levels from the surface to 0.01 hPa (~80 km).  
429 Dynamics are solved using the finite-volume dynamical core (Putman and Lin, 2007). Deep and  
430 shallow convection are parameterized using the Grell-Freitas (2014) and Park-Bretherton (2009)  
431 schemes, respectively, and moist physics is from Bacmeister et al. (2006). The turbulence  
432 parameterization is based on the non-local scheme of Lock et al. (2000). Shortwave and  
433 longwave radiative fluxes are computed in 30 bands using the Rapid Radiative Transfer Model  
434 for GCMs (RRTMG, Iacono et al. 2008).

435 Stratospheric and tropospheric chemistry are from the Global Modeling Initiative (GMI)  
436 mechanism (Duncan et al., 2007; Strahan et al., 2007; Nielsen et al., 2017), updated here to  
437 include reactions for sulfur species. The GMI mechanism in GEOSCCM has been extensively  
438 evaluated for its stratospheric ozone-related photochemistry and transport in various model  
439 intercomparisons, including Stratosphere-troposphere Processes and their Role in Climate  
440 (SPARC) Chemistry Climate Model Validation (CCMVal), CCMVal-2, and the CCM (SPARC-  
441 CCMVal, 2010; Eyring et al., 2010, 2013; Morgenstern et al., 2017). Aerosol species are



442 simulated by the Goddard Chemistry, Aerosol, Radiation, and Transport, second generation  
443 (GOCART-2G), module (Collow et al. 2024), which includes a sectional approach for dust (five  
444 bins), sea salt (five bins), and nitrate (three bins), and a bulk approach for sulfate (dimethyl  
445 sulfide, SO<sub>2</sub>, methanesulfonic acid, and SO<sub>4</sub><sup>2-</sup>) aerosol and carbonaceous species (hydrophobic  
446 and hydrophilic modes of “white” and “brown” organics and black carbon).

447 For the GEOSCCM simulations performed with the GOCART-2G module we use the  
448 nominal GOCART-2G sulfate mechanism, updated here to use the online hydroxyl (OH) radical,  
449 nitrate (NO<sub>3</sub>) radical, and hydrogen peroxide (H<sub>2</sub>O<sub>2</sub>) from the GMI mechanism instead of  
450 climatological fields provided from offline files (Collow et al., 2024). While not a full coupling  
451 to the GMI sulfur cycle it nevertheless allows the GOCART-2G sulfate mechanism to have the  
452 impact of the Hunga water vapor perturbation on the oxidants. A second “instance” of the  
453 GOCART-2G sulfate mechanism is run that is specifically for the volcanic SO<sub>2</sub> and resultant  
454 sulfate from the Hunga eruption. This allows us to track the eruptive volcanic aerosol separately  
455 from the nominal sulfate instance that sees mainly tropospheric sources. We assign this volcanic  
456 instance optical properties consistent with SAGE retrievals of the sulfate aerosol properties,  
457 using an effective radius of 0.4 microns. We find that 750 Tg of H<sub>2</sub>O is needed in the initial  
458 injection to provide a residual ~150 Tg of water in the stratosphere after a week. All other  
459 injection parameters follow the protocol. The model spinup was performed by “replaying” to the  
460 MERRA-2 meteorology (Gelaro et al. 2017), and is used throughout the **Exp2a** results.

461

#### 462 **4.6 GEOS/CARMA**

463 A second configuration of the GEOSCCM, coupled to the sectional aerosol microphysics  
464 package CARMA, also simulated the eruption (GEOS/CARMA). This configuration is the same  
465 as above except for the aerosol package and its coupling to the GMI chemistry mechanism. For  
466 this version of GEOSCCM, we use the configuration of CARMA described in Case et al. (2023).  
467 This configuration uses 24 size bins, spread logarithmically in volume between 0.25nm and  
468 6.7µm in radius and simulates the nucleation, condensational growth, evaporation, coagulation,  
469 and settling of sulfate aerosols in these simulations following the mechanism of English et al.  
470 (2013). For these simulations, CARMA is fully coupled to the GMI sulfur cycle by the  
471 production (i.e., oxidation of SO<sub>2</sub>, evaporation of sulfate aerosols) and loss (i.e., nucleation and  
472 condensation of sulfate aerosols) of sulfuric acid (H<sub>2</sub>SO<sub>4</sub>) vapor. Optical properties for the  
473 CARMA aerosols are calculated based on the interactively calculated aerosol size distribution.  
474 The same injection parameters for GEOSCCM described above are used by this configuration.  
475 This model configuration contributed to **Exp2a** and “replayed” to MERRA-2 meteorology as  
476 above.

477

#### 478 **4.7 GSFC2D**

479 The NASA/Goddard Space Flight Center two-dimensional (2D) chemistry-climate model  
480 (GSFC2D) has a domain extending from the surface to ~92 km (0.002 hPa). The model has 76  
481 levels, with 1 km vertical resolution from the surface to the lower mesosphere (60 km) and 2 km  
482 resolution above (60-92 km). The horizontal resolution is 4° latitude, and the model uses a 2D  
483 (latitude-altitude) finite volume dynamical core (Lin & Rood, 1996) for advective transport. The  
484 model has detailed stratospheric chemistry and reduced tropospheric chemistry, with a diurnal  
485 cycle computed for all constituents each day (Fleming et al., 2024). The model uses prescribed  
486 zonal mean surface temperature as a function of latitude and season based on a multi-year  
487 average of MERRA-2 data (Gelaro et al., 2017). Zonal mean latent heating, tropospheric water



488 vapor, and cloud radiative properties as a function of latitude, altitude, and season are also  
489 prescribed (Fleming et al., 2020).

490 For the free-running simulations, the model planetary wave parameterization (Bacmeister  
491 et al., 1995; Fleming et al., 2024) uses lower boundary conditions (750 hPa, ~2 km) of  
492 geopotential height amplitude and phase for zonal wave numbers 1–4. These are derived as a  
493 function of latitude and season using: 1) a 30-year average (1991–2020) of MERRA-2 data for  
494 the standard yearly-repeating climatological-dynamics simulations (“Clim-NoQBO”); and 2)  
495 individual years of MERRA-2 data (1980-2020) randomly rearranged in time to generate  
496 interannual variations in stratospheric dynamics (“ensemble1”, “ensemble2”,...“ensemble10”).  
497 For the inter-annually varying dynamics simulations, the model includes an internally generated  
498 QBO (Fleming et al., 2024).

499 For experiments that include the Hunga volcanic aerosols, the simulations go through the  
500 end of 2023, using prescribed aerosol properties for 2022-2023 from both the GloSSAC data set  
501 and derived from the OMPS-LP data (Taha et al., 2021, 2022). For experiments that include the  
502 Hunga H<sub>2</sub>O injection, Aura/MLS observations are used to derive a daily zonal mean Hunga  
503 water vapor anomaly in latitude-altitude, which is added to the baseline H<sub>2</sub>O (no volcano)  
504 through the end of February 2022. This combined water vapor field is then fully model computed  
505 starting 1 March 2022 through the end of 2031.

506 For **Exp2b**, the model zonal mean temperature and transport fields are computed from  
507 the MERRA-2 reanalysis data. These are input into the model and used as prescribed fields (no  
508 nudging is done).

509

#### 510 **4.8 IFS-COMPO**

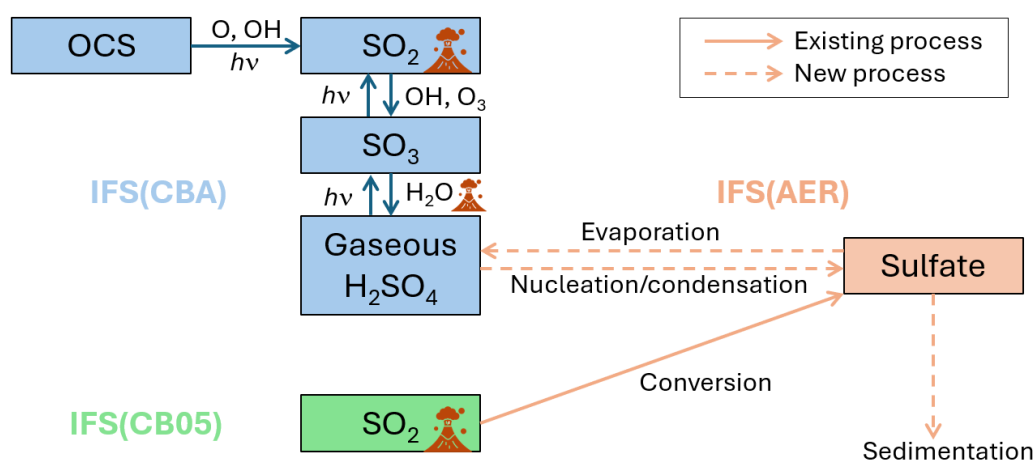
511 The Copernicus Atmosphere Monitoring Service (CAMS) provides daily global analysis  
512 and 5-day forecasts of atmospheric composition (aerosols, trace gases, and GHGs) (Peuch et al.  
513 2022). CAMS is coordinated by the European Centre for Medium Range Weather Forecasts  
514 (ECMWF) and uses, for its global component, the Integrated Forecasting System (IFS), with  
515 extensions to represent aerosols, trace, and GHGs, being called "IFS-COMPO" (also previously  
516 known as "C-IFS", Flemming et al. 2015). IFS-COMPO is composed of IFS(AER) for aerosols,  
517 as described in Remy et al. (2022) while the atmospheric chemistry is based on the chemistry  
518 module as described in Williams et al. (2022) for the troposphere (IFS-CB05) and Huijnen et al.  
519 (2016) for the stratosphere (IFS-CBA). The stratospheric chemistry module of IFS-COMPO is  
520 derived from the Belgian Assimilation System for Chemical ObErvations (BASCOE, Errera et al  
521 2019). IFS-COMPO stratospheric chemistry is used since the operational implementation of cycle  
522 48R1 on June 27, 2023 (Eskes et al., 2024).

523 The aerosol component of IFS-COMPO is a bulk aerosol scheme for all species except sea  
524 salt aerosol and desert dust, for which a sectional approach is preferred, with three bins for each  
525 of these two species. Since the implementation of operational cycle 48R1 in June 2023, the  
526 prognostic species are sea salt, desert dust, organic matter (OM), black carbon (BC), sulfate,  
527 nitrate, ammonium, and secondary organic aerosols (SOA).

528 For **Exp2a**, cycle 49R1 IFS-COMPO has been used, which will become operational for  
529 CAMS production in November 2024, at a resolution of TL511 (~40 km grid cell) over 137 model  
530 levels from surface to 0.01 hPa. Cycle 49R1 IFS-COMPO integrates a number of updates of  
531 tropospheric and stratospheric aerosols and chemistry. The most relevant aspect for this work  
532 concerns the representation of stratospheric aerosols, which has been revisited with the  
533 implementation of a coupling to the stratospheric chemistry through a simplified stratospheric



534 sulfur cycle including nucleation/condensation and evaporation processes, as shown in **Figure 4**.  
 535 Direct injection of water vapor into the stratosphere is expected to enhance the nucleation and  
 536 condensation of sulfate through the reaction with  $\text{SO}_3$  and production of gas-phase  $\text{H}_2\text{SO}_4$ .  
 537 The volcanic injection takes place between 3 and 6 UTC on January 15, 2022, with a  
 538 uniform vertical distribution between 25 and 30 km of altitude, over a rectangular region of 400  
 539 km (latitude) x 200 km (longitude) centered on the coordinates of the Hunga volcano. The injected  
 540 quantities are 0.5 Tg  $\text{SO}_2$  and 190 Tg  $\text{H}_2\text{O}$ .  
 541



542 **Figure 4.** Architecture of the stratospheric extension of IFS(AER) and its coupling with IFS(CBA)  
 543 and IFS(CB05), with existing and new processes implemented in cycle 49R1 of IFS-COMPO.  $h\nu$   
 544 represents photolysis and the volcano symbols represent direct injections by volcanic eruptions.  
 545 Sedimentation is indicated as a new process because it has been revisited.  
 546  
 547  
 548

#### 549 4.9 LMDZ6.2-LR-STRATAER and LMDZ6.2-LR-STRATAER-REPROBUS

550 The Institut Pierre-Simon Laplace Climate Modelling Centre (IPSL CMC, see  
 551 <https://cmc.ipsl.fr>) has set up a new version of its climate model in the runup of CMIP6. Further  
 552 description of the IPSL-CM6A-LR climate model can be found in Boucher et al. (2020) and in  
 553 Lurton et al. (2020). New development of the model is now ongoing to prepare the IPSLCM7  
 554 version.

555 The IPSLCM7 climate model is using the general circulation model named LMDZ for  
 556 *Laboratoire de Météorologie Dynamique-Zoom* (Hourdin et al., 2006). The LMDZ version used  
 557 for this study is based on a regular horizontal grid with 144 points regularly spaced in longitude  
 558 and 142 in latitude, corresponding to a resolution of  $2.5^\circ \times 1.3^\circ$ . The model has 79 vertical layers  
 559 and extends up to 80 km, which makes it a “high-top” model. The model shows a self-generated  
 560 quasi-biennial oscillation (QBO) whose period has been tuned to the observed one for the  
 561 present-day climate (Boucher et al., 2020).

562 The aerosol is interactively simulated in the STRATAER module using a sectional  
 563 scheme with 36 size bins. STRATAER is an improved version of the Sectional Stratospheric  
 564 Sulfate Aerosol (S3A) module (Kleinschmitt et al., 2017). It now takes into account the  
 565 photolytic conversion of  $\text{H}_2\text{SO}_4$  into  $\text{SO}_2$  in the upper stratosphere (Mills et al., 2005). The size-





566 dependent composition of H<sub>2</sub>SO<sub>4</sub>/H<sub>2</sub>O aerosols is now computed iteratively to ensure that the  
567 surface tension, density, and composition are consistent in the calculation of the Kelvin effect.  
568 The surface tension, density, H<sub>2</sub>SO<sub>4</sub> vapor pressure, and nucleation rates are calculated based on  
569 Vehkamäki et al. (2002). The version of the LMDZ6.2-LR-STRATAER atmospheric model used  
570 in the HTHH Impact project accounts for the stratospheric H<sub>2</sub>O source from methane oxidation.  
571 The chemistry is simulated using the REPROBUS (*REactive Processes Ruling the Ozone*  
572 *BUDget in the Stratosphere*) chemistry module that includes 55 chemical species and a  
573 comprehensive description of the stratospheric chemistry (Marchand et al., 2012, Lefèvre et al.,  
574 1994, Lefèvre et al., 1998).

575 For **Exp2a**, the H<sub>2</sub>O and SO<sub>2</sub> is injected at 27.5 km altitude using a Gaussian distribution  
576 and standard deviation of 2.5 km. The injection latitude ranges from 22°S to 14°S, and longitude  
577 ranges from 182°E to 186°E. The injections of H<sub>2</sub>O and SO<sub>2</sub> are 150 Tg and 0.5 Tg, respectively.

578

#### 579 **4.10 MIROC-CHASER**

580 The Model for Interdisciplinary Research On Climate - CHEMical Atmospheric general  
581 circulation model for Study of atmospheric Environment and Radiative forcing (MIROC-  
582 CHASER) version 6 (Seikiya et al. 2016) is a chemistry climate model, with a top at around 0.004  
583 hPa. The present version of MIROC-CHASER is built on MIROC6 (Tatebe et al. 2019) and has a  
584 spectral horizontal resolution of T85 (1.4° latitude × 1.4° longitude). The model has 81 vertical  
585 levels, with a vertical resolution 0.7 km in the lower stratosphere, ~1.2 km in the upper  
586 stratosphere, and ~3 km in the lower mesosphere. In the free-running simulations, the model  
587 generates QBO internally. The ensemble members have different initial conditions (January 1,  
588 2022), which are generated using slightly different nudging relaxation time during the spin-up.  
589 The aerosols are interactively simulated using a three-mode modal aerosol module (Seikiya et al.  
590 2016). The chemistry uses comprehensive troposphere-stratosphere chemistry (Watanabe et al.  
591 2011). The volcanic emission from continuously degassing volcanoes uses the emission inventory  
592 of Fioletov et al. (2022). For the explosive volcanic eruptions during the spin-up time, explosive  
593 volcanic emissions follow Carn (2022).

594 For **Exp1** fixed SST simulations, the model uses the observed SST from 10-year  
595 climatological mean from 2012 to 2021.

596 For **Exp2a**, the atmospheric temperature and winds are nudged to MERRA-2 reanalysis  
597 with a 12-hour relaxation using 3-hour meteorology. The observed SST uses the NOAA 1/4° Daily  
598 Optimum Interpolation Sea Surface Temperature (OISST) from 2022 to 2023 (Huang et al. 2020).

599 The initial volcanic injection altitude and area are not tuned but follow the experimental  
600 protocol. For **Exp1** and **Exp2a**, the H<sub>2</sub>O and SO<sub>2</sub> are injected at 25 to 30 km altitude. The injection  
601 latitude ranges from 22°S to 14°S, and longitude ranges from 182°E to 186°E. The initial injection  
602 of H<sub>2</sub>O is 186 Tg, with ~150 Tg left after the first week following the eruption. The large initial  
603 H<sub>2</sub>O injection is necessary to keep 150 Tg in the stratosphere as requested by the experimental  
604 protocol, because a large amount of ice clouds generates and falls to the troposphere soon after the  
605 eruption.

606

#### 607 **4.11 WACCM6/MAM4**

608 The Whole Atmosphere Community Climate Model version 6 (WACCM6; Gettelman et  
609 al. 2019) is the high-top version of the atmospheric component of the Community Earth System  
610 Model, version 2 (CESM2), with a top at around 140 km. WACCM6 has a horizontal resolution  
611 of 0.9° latitude × 1.25° longitude, utilizing the finite volume dynamical core (Lin & Rood,





1996). The model has 70 vertical levels, with a vertical resolution  $\sim 1$  km in the lower stratosphere,  $\sim 1.75$  km in the upper stratosphere, and  $\sim 3.5$  km in the upper mesosphere and lower thermosphere (Garcia et al., 2017). In the free-running simulations, the model generates QBO internally (Mills et al., 2017; Gettelman et al. 2019). The ensemble members differ in the last date of nudging (from January 27 to February 5, 2022). The aerosol is interactively simulated using a four-mode modal aerosol module (MAM4; Liu et al., 2012, 2016; Mills et al., 2016), in which we used the Vehkamäki nucleation scheme (Vehkamäki et al., 2002). The chemistry uses comprehensive troposphere-stratosphere-mesosphere-lower-thermosphere (TSMLT) chemistry (Gettelman et al. 2019). The volcanic emissions from continuously degassing volcanoes use the emission inventory of Andres and Kasgnoc (1998). For the explosive volcanic eruptions during the spin-up time, explosive volcanic emissions follow Mills et al. (2016) and Neely III and Schmidt (2016) with updates until 2022.

For **Exp1** and **Exp4** with the coupled ocean simulation, the ocean and sea-ice are initialized on January 3, 2022 with output from a standalone ocean model forced by atmospheric state fields and fluxes from the Japanese 55-year Reanalysis (Tsujino et al., 2018). To accurately simulate the early plume structure and evolution, the winds and temperatures in WACCM are nudged toward the Analysis for Research and Applications, MERRA-2 meteorological data (Gelaro et al., 2017) throughout January 2022. After February 1, 2022, the model is free-running to capture fully-coupled variability. For the fixed SST simulation, the model uses the 10-year climatology SST from 2012 to 2021.

For **Exp2**, the atmospheric temperature and winds are nudged to MERRA-2 reanalysis with a 12-hour relaxation using 3-hour meteorology (Davis et al., 2022). The observed SST uses 10-year climatological mean from 2012 to 2021.

The initial volcanic injection altitude and area are the same as described for section 4.1 CAM5/CARMA.

#### 4.12 WACCM6/CARMA

WACCM6/CARMA only performed **Exp2** and used a configuration similar to WACCM6/MAM4 with the same horizontal and vertical resolution, SSTs, and meteorological nudging. Differences compared to WACCM6/MAM4 are the chemistry and aerosol configuration used. WACCM6/CARMA used the middle atmosphere chemistry with limited chemistry in the troposphere and comprehensive chemistry in the stratosphere, mesosphere and lower thermosphere (Davis et al., 2022). Furthermore, we use the Community Aerosol and Radiation Model for Atmospheres (CARMA, Tilmes et al. 2023, based on Yu et al., 2015 with some updates) as the aerosol module, in which we used the Vehkamäki nucleation scheme (Vehkamäki et al., 2002). CARMA defines 20 mass bins and tracks the dry mass of the particles and assumes particle water is in equilibrium with the environmental water vapor. The approximate radius ranges from 0.2 nm to 1.3  $\mu\text{m}$  in radius for the pure sulfate group that sulfate homogeneous nucleation occurs in, and ranges from 0.05 to 8.7  $\mu\text{m}$  in the mixed group that tracks all major tropospheric aerosol types (i.e. black carbon, organic carbon, sea salt, dust, sulfate).

The initial volcanic injection altitude and area are determined by validating the water and aerosol transportation in the first six months against MLS and OMPS observations. In these



655 simulations, the H<sub>2</sub>O is injected to 25 to 35 km altitude following Zhu et al. (2022), while the SO<sub>2</sub>  
656 is injected 82% of the total mass to 26.5-28 km and 18% to 28-36 km altitude. The injection latitude  
657 ranges from 22°S to 6°S, and longitude ranges from 182.5°E to 202.5°E.

658

## 659 **5. Summary**

660 A multi-model observation comparison project is designed to evaluate the impact of the  
661 2022 Hunga eruption. Four experiments are designed to cover various research interests for this  
662 eruption, including sulfate and water plume dispersion and transport, dynamical and chemical  
663 responses in the stratosphere, and climate impact. The project will not only benefit the Hunga  
664 Impact assessment, but also benchmark the model performance on simulating stratospheric  
665 explosive volcanic eruption events. These events have a potentially large impact on the Earth  
666 system, especially on the stratospheric ozone layer and radiative balance.

667

668

### 669 **Code/Data availability**

670 GloSSAC: DOI (10.5067/GloSSAC-L3-V2.2).

671

### 672 **Author Contributions:**

673 Y.Z. Concept design, Project Administration, Experiment design, data archive, WACCM models  
674 setup;

675 E.A. provides NOAA balloon aerosol and water vapor observations for experiments

676 E.B. and S.T. and J.Z. Experiment design, conducts experiments using WACCM6MAM;

677 A.B. Experiment design, Data archive;

678 A.J. Experiment 2b prescribed fields preparation;

679 M.K. provides GloSSAC data for Exp 2b;

680 Takashi S. and S.W.: S.W. conducted all MIROC-CHASER experiments, data post-processing,  
681 data archive under supervision of Takashi S., who developed the aerosol microphysics scheme of  
682 the model.

683 X.W. and W.Y. Conducts experiment using WACCM6MAM;

684 Z.Z. Conducts experiment using WACCM6MAM, WACCM6MAM data post-processing, data  
685 archive;

686 N.L. and S.B.: Conducts experiment using IPSL7-STRATAER, data post-processing and archive

687 M.M. and L.F.: Conducts experiment using IPSL7-STRATAER-REPROBUS, data post-  
688 processing and archive

689 S.R. and S.C. Conducts experiments using IFS-COMPO

690 M.C. Experiment design, Tonga-MIP lead;

691 F.F.Ø., G.K., O.M. contributed to experiment design

692 C.B. Conducts experiment using EMAC

693 I.Q., V.A., R.U. and A.K. Model output inspection and evaluation

694 E.F. Conducts experiments using GSFC2D, data post-processing, and data archive.

695 D.P. Contributed to experiment design and conducted experiments using CMAM and data post-  
696 processing

697 P.R.C., L.D.O., Q.L., M.M., and S.S. Contributed to experiment design and conducted  
698 experiments with the NASA GEOS CCM

699 P.C. and P.R.C. Contributed to experiment design and conducted experiments with the NASA  
700 GEOS CARMA model



701 H.A. and Y.Y. Conducts experiment using CCSRNIES-MIROC3.2, data post-processing and  
702 archive  
703 D.V. contributed to experiment design and assisted E.B. with variables request  
704 W.R. and P.N. concept design  
705 G.M. concept design and in charge of JASMIN data archiving  
706 P.Y. and Y.P. conduct experiments using CAM5CARMA and data post-processing  
707 S.T. and C.-C. L. conduct experiments using WACCM6CARMA and data post-processing  
708

#### 709 **Competing interests**

710 We declare at least one of the co-authors is on the editorial board of GMD.

711

#### 712 **Acknowledgement:**

713 We acknowledge Michelle Santee, Martyn Chipperfield, Allegra Legrande, Thomas Peter,  
714 Myriam Khodri for their valuable input for this project.

715 This research has been supported by the National Oceanic and Atmospheric Administration  
716 (grant nos. 03- 01-07-001, NA17OAR4320101, and NA22OAR4320151). NCAR's Community  
717 Earth System Model project is supported by the National Center for Atmospheric Research,  
718 which is a major facility sponsored by the NSF under Cooperative Agreement No. 1852977.

719 W.Y.'s work was performed under the auspices of the U.S. Department of Energy by Lawrence  
720 Livermore National Laboratory under Contract DE-AC52-07NA27344. TS and SW were  
721 supported by MEXT-Program for the advanced studies of climate change projection (SENTAN)  
722 Grant Number JPMXD0722681344 and their MIROC-CHASER and MIROC-ES2H simulations  
723 were conducted using the Earth Simulator at JAMSTEC. IFS-Compo is supported by the  
724 Copernicus Atmosphere Monitoring Service (CAMS), which is one of six services that form  
725 Copernicus, the European Union's Earth observation programme.

726 The IPSLCM7 model experiments were performed using the high-performance computing  
727 (HPC) resources of TGCC (Très Grand Centre de Calcul) under allocations 2024-A0170102201  
728 (project gen2201) provided by GENCI (Grand Équipement National de Calcul Intensif). This  
729 study benefited from the ESPRI (Ensemble de Services Pour la Recherche l'IPSL) computing  
730 and data centre (<https://mesocentre.ipsl.fr>) which is supported by CNRS, Sorbonne Université,  
731 École Polytechnique and CNES.

732 V.A. is supported by the NASA NNH22ZDA001N-ACMAP and NNH19ZDA001N-IDS  
733 programs.

734 F.F.Ø. acknowledge support from the European Union's Horizon 2020 research and innovation  
735 programme under the Marie Skłodowska-Curie grant 891186.

736 R.U. is supported by NASA Upper Atmospheric Composition Observations and Aura Science  
737 Team programs as well as through the NASA Internal Scientist Funding Model.

738 P.R.C., L.D.O., Q.L, S.S., M.M., and P.C. are supported by the NASA Modeling Analysis and  
739 Prediction program (program manager: David Considine, NASA HQ) through the NASA  
740 Internal Scientist Funding Model. P.C. is additionally supported by the NASA Postdoctoral  
741 Program. GEOS CCM and GEOS CARMA simulations were performed at the NASA Center for  
742 Climate Simulation.

743 H.A. and Y.Y were supported by KAKENHI (JP24K00700 and JP24H00751) of the Ministry of  
744 Education, Culture, Sports, Science, and Technology, Japan, and NEC SX-AURORA  
745 TSUBASA at NIES were used to perform CCSRNIES-MIROC3.2 simulations.

746



747

748 **References:**

- 749 Akiyoshi, H., M. Kadowaki, Y. Yamashita, T. Nagatomo (2023), Dependence of column ozone  
750 on future ODSs and GHGs in the variability of 500-ensemble members. *Sci. Rep.* 13,  
751 320(1–12). <https://doi.org/10.1038/s41598-023-27635-y>
- 752 Akiyoshi, H., T. Nakamura, T. Miyasaka, M. Shiotani, and M. Suzuki (2016), A nudged  
753 chemistry-climate model simulation of chemical constituent distribution at northern high-  
754 latitude stratosphere observed by SMILES and MLS during the 2009/2010 stratospheric  
755 sudden warming, *J. Geophys. Res. Atmos.*, 121, 1361-1380, doi:10.1002/2015JD023334
- 756 Andres, R. J., and A. D. Kasgnoc (1998), A time-averaged inventory of subaerial volcanic sulfur  
757 emissions, *J. Geophys. Res.*, 103(D19), 25,251–25,261, doi:10.1029/98JD02091.
- 758 Bacmeister, J. T., Schoeberl, M. R., Summers, M. E., Rosenfield, J. E., & Zhu, X. (1995).  
759 Descent of long-lived trace gases in the winter polar vortex. *Journal of Geophysical*  
760 *Research*, 100(D6), 11669–11684. <https://doi.org/10.1029/94jd02958>
- 761 Bacmeister, J. T., Suarez, M. J., & Robertson, F. R. (2006). Rain reevaporation, boundary  
762 layer–convection interactions, and Pacific rainfall patterns in an AGCM. *Journal of the*  
763 *Atmospheric Sciences*, 63(12), 3383-3403.
- 764 Bernath, P. F., McElroy, C. T., Abrams, M. C., Boone, C. D., Butler, M., Camy-Peyret, C.,  
765 Carleer, M., Clerbaux, C., Coheur, P.-F., Colin, R., DeCola, P., DeMazière, M.,  
766 Drummond, J. R., Dufour, D., Evans, W. F. J., Fast, H., Fussen, D., Gilbert, K., Jennings,  
767 D. E., Llewellyn, E. J., Lowe, R. P., Mahieu, E., McConnell, J. C., McHugh, M., McLeod,  
768 S. D., Michaud, R., Midwinter, C., Nassar, R., Nichitiu, F., Nowlan, C., Rinsland, C. P.,  
769 Rochon, Y. J., Rowlands, N., Semeniuk, K., Simon, P., Skelton, R., Sloan, J. J., Soucy, M.-  
770 A., Strong, K., Tremblay, P., Turnbull, D., Walker, K. A., Walkty, I., Wardle, D. A.,  
771 Wehrle, V., Zander, R., and Zou, J., Atmospheric Chemistry Experiment (ACE): Mission  
772 overview, *Geophysical Research Letters*, 32, <https://doi.org/10.1029/2005GL022386>, 2005.
- 773 Boucher O., Servonnat, J., Albright, A. L., Aumont, O., Balkanski, Y., Bastrikov, V., et al.  
774 (2020). Presentation and evaluation of the IPSL-CM6A-LR climate model. *Journal of*  
775 *Advances in Modeling Earth Systems*, 12, e2019MS002010.  
776 <https://doi.org/10.1029/2019MS002010>.
- 777 Bretherton, C. S., & Park, S. (2009). A new moist turbulence parameterization in the  
778 Community Atmosphere Model. *Journal of Climate*, 22(12), 3422-3448.
- 779 Brodowsky, C., Sukhodolov, T., Feinberg, A., Höpfner, M., Peter, T., Stenke, A., & Rozanov, E.  
780 (2021). Modeling the sulfate aerosol evolution after recent moderate volcanic activity,  
781 2008–2012. *Journal of Geophysical Research: Atmospheres*, 126, e2021JD035472.  
782 <https://doi.org/10.1029/2021JD035472>
- 783 Bruehl, C., Lelieveld, J., Schalloock, J., & Rieger, L. A. (2023, December). Chemistry Climate  
784 Model Studies on the Effect of the Hunga Tonga Eruption on stratospheric Ozone in mid  
785 and high Latitudes in 2022. In *AGU Fall Meeting Abstracts* (Vol. 2023, No. 2235, pp.  
786 A21B-2235).



- 787 Carn, S., Clarisse, L., and Prata, A.: Multi-decadal satellite measurements of global volcanic  
788 degassing, *J. Volcanol. Geoth. Res.*, 311, 99–134,  
789 <https://doi.org/10.1016/j.jvolgeores.2016.01.002>, 2016.
- 790 Carn, S., Fioletov, V., McLinden, C. et al. A decade of global volcanic SO<sub>2</sub> emissions measured  
791 from space. *Sci Rep* 7, 44095 (2017). <https://doi.org/10.1038/srep44095>
- 792 Carn, S. (2022), Multi-Satellite Volcanic Sulfur Dioxide L4 Long-Term Global Database V4,  
793 Greenbelt, MD, USA, Goddard Earth Science Data and Information Services Center (GES  
794 DISC), Accessed: [6/9/2024], 10.5067/MEASURES/SO2/DATA405
- 795 Case, P., Colarco, P. R., Toon, B., Aquila, V., & Keller, C. A. (2023). Interactive  
796 stratospheric aerosol microphysics-chemistry simulations of the 1991 Pinatubo volcanic  
797 aerosols with newly coupled sectional aerosol and stratosphere-troposphere chemistry  
798 modules in the NASA GEOS Chemistry-Climate Model (CCM). *Journal of Advances in*  
799 *Modeling Earth Systems*, 15(8), e2022MS003147.
- 800 Clyne, M., Lamarque, J.-F., Mills, M. J., Khodri, M., Ball, W., Bekki, S., Dhomse, S. S., Lebas,  
801 N., Mann, G., Marshall, L., Niemeier, U., Poulain, V., Robock, A., Rozanov, E., Schmidt,  
802 A., Stenke, A., Sukhodolov, T., Timmreck, C., Toohey, M., Tummon, F., Zanchettin, D.,  
803 Zhu, Y., and Toon, O. B.: Model physics and chemistry causing intermodel disagreement  
804 within the VolMIP-Tambora Interactive Stratospheric Aerosol ensemble, *Atmos. Chem.*  
805 *Phys.*, 21, 3317–3343, <https://doi.org/10.5194/acp-21-3317-2021> , 2021.
- 806 Clyne, M.: Modeling the Role of Volcanoes in the Climate System – Chapter 4: Tonga-  
807 MIP, Ph.D. dissertation, University of Colorado at Boulder, ProQuest Dissertations &  
808 Theses, 31487034, 153 pp., 2024.
- 809 A. Collopy, P. Colarco, A. da Silva, V. Buchard, H. Bian, M. Chin, S. Das, R. Govindaraju,  
810 D. Kim, V. Aquila: Benchmarking GOCART-2G in the Goddard Earth Observing System  
811 (GEOS), *Geoscientific Model Development*, 17, 1443–1468, doi: 10.5194/gmd-17-1443-  
812 2024 (2024).
- 813 Davis, N. A., Callaghan, P., Simpson, I. R., and Tilmes, S.: Specified dynamics scheme impacts  
814 on wave-mean flow dynamics, convection, and tracer transport in CESM2 (WACCM6),  
815 *Atmos. Chem. Phys.*, 22, 197–214, <https://doi.org/10.5194/acp-22-197-2022>, 2022.
- 816 Dhomse, S. S., Mann, G. W., Antuña Marrero, J. C., Shallcross, S. E., Chipperfield, M. P.,  
817 Carslaw, K. S., Marshall, L., Abraham, N. L., and Johnson, C. E.: Evaluating the simulated  
818 radiative forcings, aerosol properties, and stratospheric warmings from the 1963 Mt Agung,  
819 1982 El Chichón, and 1991 Mt Pinatubo volcanic aerosol clouds, *Atmos. Chem. Phys.*, 20,  
820 13627–13654, <https://doi.org/10.5194/acp-20-13627-2020>, 2020.
- 821 Duncan, B. N., Logan, J. A., Bey, I., Megretskaya, I. A., Yantosca, R. M., Novelli, P. C., ...  
822 & Rinsland, C. P. (2007). Global budget of CO, 1988–1997: Source estimates and  
823 validation with a global model. *Journal of Geophysical Research: Atmospheres*, 112(D22).
- 824 English, J. M., Toon, O. B., Mills, M. J., and Yu, F.: Microphysical simulations of new particle  
825 formation in the upper troposphere and lower stratosphere, *Atmos. Chem. Phys.*, 11, 9303-  
826 9322, 10.5194/acp-11-9303-2011, 2011.





- 827 English, J. M., Toon, O. B., & Mills, M. J. (2013). Microphysical simulations of large  
828 volcanic eruptions: Pinatubo and Toba. *Journal of Geophysical Research: Atmospheres*,  
829 *118*(4), 1880-1895.
- 830 Errera, Q., Chabrillat, S., Christophe, Y., Deboscher, J., Hubert, D., Lahoz, W., Santee, M. L.,  
831 Shiotani, M., Skachko, S., von Clarmann, T., and Walker, K.: Technical note: Reanalysis  
832 of Aura MLS chemical observations, *Atmos. Chem. Phys.*, *19*, 13647–13679,  
833 <https://doi.org/10.5194/acp-19-13647-2019>, 2019.
- 834 Eskes, H., Tsikerdekis, A., Ades, M., Alexe, M., Benedictow, A. C., Bennaoui, Y., Blake,  
835 L., Bouarar, I., Chabrillat, S., Engelen, R., Errera, Q., Flemming, J., Garrigues, S.,  
836 Griesfeller, J., Huijnen, V., Ilić, L., Inness, A., Kapsomenakis, J., Kipling, Z., Langerock,  
837 B., Mortier, A., Parrington, M., Pison, I., Pitkänen, M., Remy, S., Richter, A., Schoenhardt,  
838 A., Schulz, M., Thouret, V., Warneke, T., Zerefos, C., and Peuch, V.-H.: Technical note:  
839 Evaluation of the Copernicus Atmosphere Monitoring Service Cy48R1 upgrade of June  
840 2023, *Atmos. Chem. Phys.*, *24*, 9475–9514, <https://doi.org/10.5194/acp-24-9475-2024>,  
841 2024.
- 842 Eyring, V., Cionni, I., Bodeker, G. E., Charlton-Perez, A. J., Kinnison, D. E., Scinocca, J.  
843 F., ... & Yamashita, Y. (2010). Multi-model assessment of stratospheric ozone return dates  
844 and ozone recovery in CCMVal-2 models. *Atmospheric Chemistry and Physics*, *10*(19),  
845 9451-9472. <https://doi.org/10.5194/acp-10-9451-2010>
- 846 Fioletov, V., McLinden, C. A., Griffin, D., Abboud, I., Krotkov, N., Leonard, P. J. T., Li, C.,  
847 Joiner, J., Theys, N., and Carn, S. (2022), Multi-Satellite Air Quality Sulfur Dioxide (SO<sub>2</sub>)  
848 Database Long-Term L4 Global V2, Edited by Peter Leonard, Greenbelt, MD, USA,  
849 Goddard Earth Science Data and Information Services Center (GES DISC), Accessed:  
850 [6/9/2024], 10.5067/MEASURES/SO2/DATA406
- 851 Fleming, E. L., Newman, P. A., Liang, Q., & Daniel, J. S. (2020). The impact of continuing  
852 CFC-11 emissions on stratospheric ozone. *Journal of Geophysical Research: Atmospheres*,  
853 *125*(3), e2019JD031849. <https://doi.org/10.1029/2019jd031849>
- 854 Fleming, E. L., Newman, P. A., Liang, Q., & Oman, L. D. (2024). Stratospheric temperature and  
855 ozone impacts of the Hunga Tonga-Hunga Ha'apai water vapor injection. *Journal of*  
856 *Geophysical Research: Atmospheres*, *129*(1), e2023JD039298.  
857 <https://doi.org/10.1029/2023JD039298>
- 858 Flemming, J., Huijnen, V., Arteta, J., Bechtold, P., Beljaars, A., Blechschmidt, A.-M.,  
859 Diamantakis, M., Engelen, R. J., Gaudel, A., Inness, A., Jones, L., Josse, B., Katragkou, E.,  
860 Marecal, V., Peuch, V.-H., Richter, A., Schultz, M. G., Stein, O., and Tsikerdekis, A.:  
861 Tropospheric chemistry in the Integrated Forecasting System of ECMWF, *Geosci. Model*  
862 *Dev.*, *8*, 975–1003, 2015.685 <https://doi.org/10.5194/gmd-8-975-2015>
- 863 Fomichev, V. I., Fu, C., de Grandpre, J., Beagley, S. R., Ogibalov, V. P., and McConnell, J. C.:  
864 Model thermal response to minor radiative energy sources and sinks in the middle  
865 atmosphere, *J. Geophys. Res.*, *109*, D19107, doi:10.1029/2004JD004892, 2004.





- 866 Gelaro, R., and Coauthors, 2017: The Modern-Era Retrospective Analysis for Research and  
867 Applications, Version 2 (MERRA-2). *J. Climate*, 30, 5419–5454,  
868 <https://doi.org/10.1175/JCLI-D-16-0758.1>.
- 869 Gettelman, A., Mills, M. J., Kinnison, D. E., Garcia, R. R., Smith, A. K., Marsh, D. R., Tilmes,  
870 S., Vitt, F., Bardeen, C. G., McInerney, J., Liu, H.-L., Solomon, S. C., Polvani, L. M.,  
871 Emmons, L. K., Lamarque, J.-F., Richter, J. H., Glanville, A. S., Bacmeister, J. T., Phillips,  
872 A. S., Neale, R. B., Simpson, I. R., DuVivier, A. K., Hodzic, A., and Randel, W. J.: The  
873 Whole Atmosphere Community Climate Model Version6 (WACCM6), *J. Geophys. Res.-*  
874 *Atmos.*, 124, 12380–12403, <https://doi.org/10.1029/2019JD030943>, 2019.
- 875 Gidden, M. J., Riahi, K., Smith, S. J., Fujimori, S., Luderer, G., Kriegler, E., ... & Takahashi, K.  
876 (2019). Global emissions pathways under different socioeconomic scenarios for use in  
877 CMIP6: a dataset of harmonized emissions trajectories through the end of the century.  
878 *Geoscientific model development*, 12(4), 1443-1475. [https://doi.org/10.5194/gmd-12-1443-](https://doi.org/10.5194/gmd-12-1443-2019)  
879 [2019](https://doi.org/10.5194/gmd-12-1443-2019)
- 880 Grell, G. A., & Freitas, S. R. (2014). A scale and aerosol aware stochastic convective  
881 parameterization for weather and air quality modeling. *Atmospheric Chemistry and*  
882 *Physics*, 14(10), 5233-5250. <https://doi.org/10.5194/acp-14-5233-2014>
- 883 Hersbach H, Bell B, Berrisford P, et al. (2020). The ERA5 global reanalysis. *Quarterly Journal*  
884 *of the Royal Meteorological Society*, 146: 1999–2049. <https://doi.org/10.1002/qj.3803>
- 885 Hourdin, F., Musat, I., Bony, S., Braconnot, P., Codron, F., Dufresne, J.-L., Fairhead, L.,  
886 Filiberti, M.-A., Friedlingstein, P., Grandpeix, J.-Y., Krinner, G., Levan, P., Li, Z.-X., and  
887 Lott, F.. The LMDZ4 general circulation model : climate performance and sensitivity to  
888 parametrized physics with emphasis on tropical convection. *Climate Dynamics*, 27 :787–  
889 813, 2006.
- 890 Huang, B., C. Liu, V. Banzon, E. Freeman, G. Graham, B. Hankins, T. Smith, and H.-M. Zhang,  
891 2020: Improvements of the Daily Optimum Interpolation Sea Surface Temperature  
892 (DOISST) Version 2.1, *Journal of Climate*, 34, 2923-2939. doi: 10.1175/JCLI-D-20-0166.1
- 893 Huijnen, V., Flemming, J., Chabrillat, S., Errera, Q., Christophe, Y., Blechschmidt, A.-M.,  
894 Richter, A., and Eskes, H.: C-IFS-CB05-BASCOE: stratospheric chemistry in the  
895 Integrated Forecasting System of ECMWF, *Geoscientific Model Development*, 9, 3071–  
896 3091, 2016.705
- 897 Hurrell, J. W., et al. (2013), The community Earth system model: A framework for  
898 collaborative research, *Bull. Am. Meteorol. Soc.*, doi:10.1175/BAMS-D-12-00121.
- 899 Iacono, M. J., Delamere, J. S., Mlawer, E. J., Shephard, M. W., Clough, S. A., & Collins,  
900 W. D. (2008). Radiative forcing by long-lived greenhouse gases: Calculations with the  
901 AER radiative transfer models. *Journal of Geophysical Research: Atmospheres*, 113(D13).
- 902 Jöckel, P., Kerkweg, A., Pozzer, A., Sander, R., Tost, H., Riede, H., Baumgaertner, A.,  
903 Gromov, S., and Kern, B.: Development cycle 2 of the Modular Earth Submodel System  
904 (MESSy2), *Geosci. Model Dev.*, 3, 717–752, 2010.



- 905 Jones, A. C., J. M. Haywood, A. Jones, V. Aquila. Sensitivity of volcanic aerosol  
906 dispersion to meteorological conditions: a Pinatubo case study, *J. Geophys. Res.*, 121(12),  
907 6892-6908, doi: 10.1002/2016JD025001, 2016.
- 908 Jonsson, A. I., de Grandpré, J., Fomichev, V. I., McConnell, J. C., and Beagley, S. R.,  
909 Doubled CO<sub>2</sub>-induced cooling in the middle atmosphere: Photochemical analysis of the  
910 ozone radiative feedback, *J. Geophys. Res.*, 109, D24103, doi:10.1029/2004JD005093,  
911 2004.
- 912 Kawamiya, M., Hajima, T., Tachiiri, K. et al. Two decades of Earth system modeling with an  
913 emphasis on Model for Interdisciplinary Research on Climate (MIROC). *Prog Earth Planet*  
914 *Sci* 7, 64. <https://doi.org/10.1186/s40645-020-00369-5>, (2020).
- 915 Kleinschmitt, C., Boucher, O., Bekki, S., Lott, F., and Platt, U.: The Sectional Stratospheric  
916 Sulfate Aerosol module (S3A-v1) within the LMDZ general circulation model: description  
917 and evaluation against stratospheric aerosol observations, *Geosci. Model Dev.*, 10, 3359–  
918 3378, 2017, <https://doi.org/10.5194/gmd-10-3359-2017>.
- 919 Kohl, M., C. Brühl, J. Schalloock, H. Tost, P. Jöckel, A. Jost, S. Beirle, M. Höpfner, and A.  
920 Pozzer (2024). New submodel for emissions from Explosive Volcanic ERuptions (EVER  
921 v1.1) within the Modular Earth Submodel System (MESSy, version 2.55.1),  
922 <https://doi.org/10.5194/egusphere-2024-2200>.
- 923 Lamarque, J.-F., et al. (2012), CAM-chem: Description and evaluation of interactive  
924 atmospheric chemistry in the Community Earth System Model, *Geosci. Model Dev.*, 5(2),  
925 369–411, doi:10.5194/gmd-5-369-2012.
- 926 Lefèvre, F., Brasseur, G. P., Folkins, I., Smith, A. K., and Simon, P.: Chemistry of the  
927 1991–1992 stratospheric winter: Three-dimensional model simulations, *J. Geophys. Res.-*  
928 *Atmos.*, 99, 8183–8195, <https://doi.org/10.1029/93JD03476>, 1994.
- 929 Lefèvre, F., Figarol, F., Carslaw, K. S., and Peter, T.: The 1997 Arctic Ozone depletion  
930 quantified from three-dimensional model simulations, *Geophys. Res. Lett.*, 25, 2425–2428,  
931 <https://doi.org/10.1029/98GL51812>, 1998.
- 932 Li, C., Peng, Y., Asher, E., Baron, A. A., Todt, M., Thornberry, T. D., et al. (2024).  
933 Microphysical simulation of the 2022 Hunga volcano eruption using a sectional aerosol  
934 model. *Geophysical Research Letters*, 51, e2024GL108522.  
935 <https://doi.org/10.1029/2024GL108522>
- 936 Lin, S. J., & Rood, R. B. (1996). Multidimensional flux-form semi-Lagrangian transport  
937 schemes. *Monthly weather review*, 124(9), 2046-2070. [https://doi.org/10.1175/1520-0493\(1996\)124%3C2046:MFFSLT%3E2.0.CO;2](https://doi.org/10.1175/1520-0493(1996)124%3C2046:MFFSLT%3E2.0.CO;2)
- 938  
939 Liu, X., Easter, R. C., Ghan, S. J., Zaveri, R., Rasch, P., Shi, X., Lamarque, J.-F., Gettelman, A.,  
940 Morrison, H., Vitt, F., Conley, A., Park, S., Neale, R., Hannay, C., Ekman, A. M. L., Hess,  
941 P., Mahowald, N., Collins, W., Iacono, M. J., Bretherton, C. S., Flanner, M. G., and  
942 Mitchell, D.: Toward a minimal representation of aerosols in climate models: description  
943 and evaluation in the Community Atmosphere Model CAM5, *Geosci. Model Dev.*, 5, 709–  
944 739, <https://doi.org/10.5194/gmd-5-709-2012>, 2012.



- 945 Liu, X., Ma, P.-L., Wang, H., Tilmes, S., Singh, B., Easter, R. C., Ghan, S. J., and Rasch, P. J.:  
946 Description and evaluation of a new four-mode version of the Modal Aerosol Module  
947 (MAM4) within version 5.3 of the Community Atmosphere Model, *Geosci. Model Dev.*, 9,  
948 505–522, <https://doi.org/10.5194/gmd-9-505-2016>, 2016.
- 949 Lock, A. P., Brown, A. R., Bush, M. R., Martin, G. M., & Smith, R. N. B. (2000). A new  
950 boundary layer mixing scheme. Part I: Scheme description and single-column model tests.  
951 *Monthly weather review*, 128(9), 3187-3199.
- 952 Lurton, T., Balkanski, Y., Bastrikov, V., Bekki, S., Bopp, L., Braconnot, P., et al. (2020).  
953 Implementation of the CMIP6 forcing data in the IPSL-CM6A-LR model. *Journal of*  
954 *Advances in Modeling Earth Systems*, 12, e2019MS001940.  
955 <https://doi.org/10.1029/2019MS001940>
- 956 Marchand, M., Keckhut, P., Lefebvre, S., Claud, C., Cugnet, D., Hauchecorne, A., et al. (2012).  
957 Dynamical amplification of the stratospheric solar response simulated with the Chemistry-  
958 Climate Model LMDz-Reprobus. *Journal of Atmospheric and Solar-Terrestrial Physics*,  
959 75–76, 147–160. <https://doi.org/10.1016/j.jastp.2011.11.008>
- 960 Mills, M. J., O. B. Toon, V. Vaida, P. E. Hintze, H. G. Kjaergaard, D. P. Schofield, and T. W.  
961 Robinson (2005), Photolysis of sulfuric acid vapor by visible light as a source of the polar  
962 stratospheric CN layer, *J. Geophys. Res.*, 110, D08201, doi:10.1029/2004JD005519.
- 963 Mills, M. J., Schmidt, A., Easter, R., Solomon, S., Kinnison, D. E., Ghan, S. J., Neely, R. R.,  
964 Marsh, D. R., Conley, A., Bardeen, C. G., and Gettelman, A.: Global volcanic aerosol  
965 properties derived from emissions, 1990–2014, using CESM1(WACCM), *J. Geophys.*  
966 *Res.-Atmos.*, 121, 2332–2348, <https://doi.org/10.1002/2015JD024290>, 2016.
- 967 Mills, M. J., Richter, J. H., Tilmes, S., Kravitz, B., Mac-Martin, D. G., Glanville, A. A., Tribbia,  
968 J. J., Lamarque, J.-F., Vitt, F., Schmidt, A., Gettelman, A., Hannay, C., Bacmeister, J. T.,  
969 and Kinnison, D. E.: Radiative and chemical response to interactive stratospheric sulfate  
970 aerosols in fully coupled CESM1(WACCM), *J. Geophys. Res.-Atmos.*, 122, 13061–13078,  
971 <https://doi.org/10.1002/2017JD027006>, 2017.
- 972 Molod, A., Takacs, L., Suarez, M., and Bacmeister, J.: Development of the GEOS-5 atmospheric  
973 general circulation model: evolution from MERRA to MERRA2, *Geosci. Model Dev.*, 8,  
974 1339-1356, [10.5194/gmd-8-1339-2015](https://doi.org/10.5194/gmd-8-1339-2015), 2015.
- 975 Morgenstern, O., Hegglin, M. I., Rozanov, E., O'Connor, F. M., Abraham, N. L., Akiyoshi,  
976 H., ... & Zeng, G. (2017). Review of the global models used within phase 1 of the  
977 Chemistry–Climate Model Initiative (CCMI). *Geoscientific Model Development*, 10(2),  
978 639-671.
- 979 Naujokat, B., An update of the observed Quasi-Biennial Oscillation of the stratospheric winds  
980 over the tropics, *J. Atmos. Sci.*, 43, 1873 - 1877, [https://doi.org/10.1175/1520-0469\(1986\)043<1873:AUOTOQ>2.0.CO;2](https://doi.org/10.1175/1520-0469(1986)043<1873:AUOTOQ>2.0.CO;2), 1986.
- 981 Neely III, Ryan R. and Schmidt, Anja (2016) *VolcanEESM: Global volcanic sulphur dioxide*  
982 *(SO<sub>2</sub>) emissions database from 1850 to present*. Centre for Environmental Data Analysis.  
983 [Dataset] <https://doi.org/10.5285/76ebdc0b-0eed-4f70-b89e-55e606bcd568>



- 985 Nielsen, J. E., Pawson, S., Molod, A., Auer, B., Da Silva, A. M., Douglass, A. R., ... &  
986 Wargan, K. (2017). Chemical mechanisms and their applications in the Goddard Earth  
987 Observing System (GEOS) earth system model. *Journal of Advances in Modeling Earth*  
988 *Systems*, 9(8), 3019-3044.
- 989 Peuch, V.-H., Engelen, R., Rixen, M., Dee, D., Flemming, J., Suttie, M., Ades, M., Agusti-  
990 Panareda, A., Ananasso, C., Andersson, E., Armstrong, D., Barre, J., Bousserez, N.,  
991 Dominguez, J. J., Garrigues, S., Inness, A., Jones, L., Kipling, Z., Letertre-Danczak, J.,  
992 Parrington, M., Razinger, M., Ribas, R., Vermoote, S., Yang, X., Simmons, A., de  
993 Marcilla, J. G., and Thepaut, J.-N.: The Copernicus Atmosphere Monitoring Service: From  
994 Research to Operations, *Bulletin of the American Meteorological Society*, 103, E2650 –  
995 E2668, <https://doi.org/10.1175/BAMS-D-21-0314.1>, 2022.
- 996 Pringle, K. J., Tost, H., Message, S., Steil, B., Giannadaki, D., Nenes, A., Fountoukis, C.,  
997 Stier, P., Vignati, E., and Lelieveld, J.: Description and evaluation of GMXe: a new aerosol  
998 submodel for global simulations (v1), *Geosci. Model Dev.*, 3, 391–412, 2010.
- 999 Putman, W. M., & Lin, S. J. (2007). Finite-volume transport on various cubed-sphere grids.  
1000 *Journal of Computational Physics*, 227(1), 55-78.
- 1001 Quaglia, I., Timmreck, C., Niemeier, U., Visioni, D., Pitari, G., Brodowsky, C., Brühl, C.,  
1002 Dhomse, S. S., Franke, H., Laakso, A., Mann, G. W., Rozanov, E., and Sukhodolov, T.:  
1003 Interactive stratospheric aerosol models' response to different amounts and altitudes of SO<sub>2</sub>  
1004 injection during the 1991 Pinatubo eruption, *Atmos. Chem. Phys.*, 23, 921–948,  
1005 <https://doi.org/10.5194/acp-23-921-2023>, 2023.
- 1006 Randel et al (2024): Randel, William J., Xinyue Wang, Jon Starr, Rolando R. Garcia, and  
1007 Douglas Edward Kinnison. "Long-term temperature impacts of the Hunga volcanic  
1008 eruption in the stratosphere and above." *ESS Open Archive eprints* 815 (2024):  
1009 172249118-81591303.
- 1010 Reinecker, M., Suarez, M., Todling, R., Bacmeister, J., Takacs, L., & Liu, H. (2008). The  
1011 GEOS-5 data assimilation system-documentation of versions 5.0. 1, 5.1. 0 (No. NASA  
1012 Tech Rep TM-2007, 104606).
- 1013 Rémy, S., Kipling, Z., Huijnen, V., Flemming, J., Nabat, P., Michou, M., Ades, M., Engelen, R.,  
1014 and Peuch, V.-H.: Description and evaluation of the tropospheric aerosol scheme in the  
1015 Integrated Forecasting System (IFS-AER, cycle 47R1) of ECMWF, *Geoscientific Model*  
1016 *Development*, 15, 4881–4912, <https://doi.org/10.5194/gmd-15-4881-2022>, 2022.
- 1017 Schallock, J., C. Brühl, C. Bingen, M. Höpfner, L. Rieger, and J. Lelieveld (2023),  
1018 Reconstructing volcanic radiative forcing since 1990, using a comprehensive emission  
1019 inventory and spatially resolved sulfur injections from satellite data in a chemistry-climate  
1020 model, *Atmos. Chem. Phys.*, 23, 1169–1207.
- 1021 Scinocca, J. F.: An Accurate Spectral Non-Orographic Gravity Wave Parameterization for  
1022 General Circulation Models, *J. Atmos. Sci.*, 60, 667–682, [https://doi.org/10.1175/1520-0469\(2003\)060%3C0667:AASNGW%3E2.0.CO;2](https://doi.org/10.1175/1520-0469(2003)060%3C0667:AASNGW%3E2.0.CO;2), 2003.



- 1024 Scinocca, J. F., McFarlane, N. A., Lazare, M, Li, J., and Plummer, D., Technical Note: The  
1025 CCCma third generation AGCM and its extension into the middle atmosphere, *Atmos.*  
1026 *Chem. Phys.*, 8, 7055–7074, <https://doi.org/10.5194/acp-8-7055-2008>, 2008.
- 1027 Seddon, J., Stephens, A., Mizieliński, M. S., Vidale, P. L., and Roberts, M. J.: Technology to aid  
1028 the analysis of large-volume multi-institute climate model output at a central analysis  
1029 facility (PRIMAVERA Data Management Tool V2.10), *Geosci. Model Dev.*, 16, 6689–  
1030 6700, <https://doi.org/10.5194/gmd-16-6689-2023>, 2023.
- 1031 Sekiya, T., K. Sudo, and T. Nagai (2016), Evolution of stratospheric sulfate aerosol from the  
1032 1991 Pinatubo eruption: Roles of aerosol microphysical processes, *J. Geophys. Res.*  
1033 *Atmos.*, 121, 2911–2938, doi:10.1002/2015JD024313.
- 1034 Strahan, S. E., Duncan, B. N., & Hoor, P. (2007). Observationally derived transport  
1035 diagnostics for the lowermost stratosphere and their application to the GMI chemistry and  
1036 transport model. *Atmospheric Chemistry and Physics*, 7(9), 2435-2445.
- 1037 Sukhodolov, T., Egorova, T., Stenke, A., Ball, W. T., Brodowsky, C., Chiodo, G., Feinberg, A.,  
1038 Friedel, M., Karagodin-Doyennel, A., Peter, T., Sedlacek, J., Vattioni, S., and Rozanov, E.:  
1039 Atmosphere ocean aerosol chemistry climate model SOCOLv4.0: description and  
1040 evaluation, *Geosci. Model Dev.*, 14, 5525–5560, [https://doi.org/10.5194/gmd-14-5525-](https://doi.org/10.5194/gmd-14-5525-2021)  
1041 [2021](https://doi.org/10.5194/gmd-14-5525-2021), 2021.
- 1042 Taha, G., et al. (2021), OMPS LP Version 2.0 multi-wavelength aerosol extinction coefficient  
1043 retrieval algorithm, *Atmospheric Measurement Techniques*, 14,  
1044 <https://doi.org/10.5194/amt-14-1015-2021>
- 1045 Taha, G., et al. "Tracking the 2022 Hunga Tonga-Hunga Ha'apai aerosol cloud in the upper and  
1046 middle stratosphere using space-based observations." *Geophysical Research Letters* 49.19  
1047 (2022): e2022GL100091.
- 1048 Tilmes, S., Mills, M. J., Zhu, Y., Bardeen, C. G., Vitt, F., Yu, P., Fillmore, D., Liu, X., Toon, B.,  
1049 and Deshler, T.: Description and performance of a sectional aerosol microphysical model  
1050 in the Community Earth System Model (CESM2), *Geosci. Model Dev.*, 16, 6087-6125,  
1051 [10.5194/gmd-16-6087-2023](https://doi.org/10.5194/gmd-16-6087-2023), 2023. doi: 10.5194/gmd-16-6087-2023
- 1052 Tatebe, H., Ogura, T., Nitta, T., Komuro, Y., Ogochi, K., Takemura, T., Sudo, K., Sekiguchi, M.,  
1053 Abe, M., Saito, F., Chikira, M., Watanabe, S., Mori, M., Hirota, N., Kawatani, Y.,  
1054 Mochizuki, T., Yoshimura, K., Takata, K., O'ishi, R., Yamazaki, D., Suzuki, T., Kurogi,  
1055 M., Kataoka, T., Watanabe, M., and Kimoto, M.: Description and basic evaluation of  
1056 simulated mean state, internal variability, and climate sensitivity in MIROC6, *Geosci.*  
1057 *Model Dev.*, 12, 2727–2765, <https://doi.org/10.5194/gmd-12-2727-2019>, 2019.
- 1058 Tsujino, H. et al. JRA-55 based surface dataset for driving ocean–sea-ice models (JRA55-do).  
1059 *Ocean Modell.* 130, 79–139 (2018).
- 1060 Thomason, L. W., N. Ernest, L. Millán, L. Rieger, A. Bourassa, J.-P. Vernier, G. Manney, T.  
1061 Peter, B. Luo, and F. Arfeuille (2018), A global, space-based stratospheric aerosol  
1062 climatology: 1979 to 2016, submitted to *Earth System Science Data*, 10, 469–492,  
1063 <https://doi.org/10.5194/essd-10-469-2018>.





- 1064 Kovilakam, M., Thomason, L. W., Ernest, N., Rieger, L., Bourassa, A., and Millán, L. (2020),  
1065 The Global Space-based Stratospheric Aerosol Climatology (version 2.0): 1979–2018,  
1066 Earth Syst. Sci. Data, 12, 2607–2634, <https://doi.org/10.5194/essd-12-2607-2020>.
- 1067 Kovilakam, M., Thomason, L., and Knepp, T.: SAGE III/ISS aerosol/cloud categorization and its  
1068 impact on GloSSAC, Atmos. Meas. Tech., 16, 2709–2731, [https://doi.org/10.5194/amt-16-](https://doi.org/10.5194/amt-16-2709-2023)  
1069 [2709-2023](https://doi.org/10.5194/amt-16-2709-2023), 2023.
- 1070 Vehkamäki, H., Kulmala, M., Napari, I., Lehtinen, K. E., Timmreck, C., Noppel, M., and  
1071 Laaksonen, A.: An improved parameterization for sulfuric acid-water nucleation rates for  
1072 tropospheric and stratospheric conditions, J. Geophys. Res.-Atmos., 107, AAC 3- 1–AAC  
1073 3-10, <https://doi.org/10.1029/2002JD002184>, 2002.
- 1074 Wang, X., Randel, W., Zhu, Y., Tilmes, S., Starr, J., Yu, W., et al. (2023). Stratospheric climate  
1075 anomalies and ozone loss caused by the Hunga Tonga-Hunga Ha'apai volcanic eruption.  
1076 Journal of Geophysical Research: Atmospheres, 128, e2023JD039480.  
1077 <https://doi.org/10.1029/2023JD039480>
- 1078 Watanabe, S., Hajima, T., Sudo, K., Nagashima, T., Takemura, T., Okajima, H., Nozawa, T.,  
1079 Kawase, H., Abe, M., Yokohata, T., Ise, T., Sato, H., Kato, E., Takata, K., Emori, S., and  
1080 Kawamiya, M.: MIROC-ESM 2010: model description and basic results of CMIP5-20c3m  
1081 experiments, Geosci. Model Dev., 4, 845–872, <https://doi.org/10.5194/gmd-4-845-2011>,  
1082 2011.
- 1083 Williams, J. E., Huijnen, V., Bouarar, I., Meziane, M., Schreurs, T., Pelletier, S., Marecal, V.,  
1084 Josse, B., and Flemming, J.: Regional evaluation of the performance of the global CAMS  
1085 chemical modeling system over the United States (IFS cycle 47r1), Geoscientific Model  
1086 Development, 15, 4657–4687, <https://doi.org/10.5194/gmd-15-4657-2022>, 2022.
- 1087 Yu, P., O. B. Toon, C. G. Bardeen, M. J. Mills, T. Fan, J. M. English, and R. R. Neely (2015),  
1088 Evaluations of tropospheric aerosol properties simulated by the community earth system  
1089 model with a sectional aerosol microphysics scheme, J. Adv. Model. Earth Syst., 7, 865–  
1090 914, doi:10.1002/2014MS000421.
- 1091 Yu, W., Garcia, R., Yue, J., Smith, A., Wang, X., Randel, W., ... & Mlynczak, M. (2023).  
1092 Mesospheric temperature and circulation response to the Hunga Tonga-Hunga-Ha'apai  
1093 volcanic eruption. Journal of Geophysical Research: Atmospheres, 128(21),  
1094 e2023JD039636.
- 1095 Zhang, J., Kinnison, D., Zhu, Y., Wang, X., Tilmes, S., Dube, K., & Randel, W. (2024).  
1096 Chemistry contribution to stratospheric ozone depletion after the unprecedented water-rich  
1097 Hunga Tonga eruption. Geophysical Research Letters, 51, e2023GL105762.  
1098 <https://doi.org/10.1029/2023GL105762>
- 1099 Zhou, X., S.S. Dhomse, W. Feng, G. Mann, S. Heddell, H. Pumphrey, B.J. Kerridge, B.  
1100 Latter, R. Siddans, L. Ventress, R. Querel, P. Smale, E. Asher, E.G. Hall, S. Bekki and  
1101 M.P. Chipperfield (2024), Antarctic vortex dehydration in 2023 as a substantial removal  
1102 pathway for Hunga Tonga-Hunga Ha'apai water vapour, Geophysical Research Letters, 51,  
1103 e2023GL107630, [doi:10.1029/2023GL107630](https://doi.org/10.1029/2023GL107630).





1104 Zhu, Y., Bardeen, C.G., Tilmes, S. et al. Perturbations in stratospheric aerosol evolution due to  
1105 the water-rich plume of the 2022 Hunga-Tonga eruption. *Commun Earth Environ* 3, 248  
1106 (2022). <https://doi.org/10.1038/s43247-022-00580-w>